

University of South Bohemia in České Budějovice
Faculty of Science

Utilising CRISPR-Cas9 mediated genome editing to C-terminally tag endogenous gene loci with fluorescent protein fusions in preimplantation mouse embryos

Master's thesis

Bc. Miriama Peřanská

Supervisor: doc. Alexander W. Bruce, Ph.D.

České Budějovice 2020

Master's thesis

Pekřanská M., 2020: Utilising CRISPR-Cas9 mediated genome editing to C-terminally tag endogenous gene loci with fluorescent protein fusions in preimplantation mouse embryos. Mgr. Thesis, in English. – 82 p., Faculty of Science, University of South Bohemia, České Budějovice, Czech Republic.

Annotation

Master's thesis demonstrates the C-terminally fluorescent tagging of endogenous genes in the preimplantation mouse embryos by utilizing CRISPR-Cas9 mediated genome editing method.

Financial sources: GACR: 18-02891S

I hereby proclaim that I wrote my master's thesis on my own under the leadership of my supervisor and that the references include all resources and literature I have used.

I hereby declare that, in accordance with Article 47b of Act No. 111/1998 in the valid wording, I agree with the publication of my master's thesis, in full form to be kept in the Faculty of Science archive, in electronic form in publicly accessible part of the STAG database operated by the University of South Bohemia in České Budějovice accessible through its web pages.

Further, I agree to the electronic publication of the comments of my supervisor and thesis opponents and the record of the proceedings and results of the thesis defense in accordance with aforementioned Act No. 111/1998. I also agree to the comparison of the text of my thesis with the Theses.cz thesis database operated by the National Registry of University Theses and a plagiarism detection system.

České Budějovice, 9.12.2020

Acknowledgements

First and foremost, my big gratitude goes to my supervisor doc. Alexander W. Bruce, Ph.D. Thank you for the opportunity to perform my master research in your laboratory. I really appreciate your guidance during the time spent in your team, it was truly a most enriching time, during which I gained valuable knowledge and important practical skills in molecular and developmental biology.

Secondly, I would like to thank my colleagues for their help, advice and cooperation. My thanks belong to Rebecca Collier M.Sc. (Ph.D. student), who was always more than willing to help me with the embryo work and performed the microinjections. I honestly could not wish for better teacher and advisor who shared all the best techniques and invaluable information with me. Thank you for your time and good ideas. Next, I would like to thank Mgr. Lenka Gahurová, Ph.D. for her friendship and her clear explanations and answers to all my questions. Mgr. Martina Stiborova, Giorgio Virnicchi, M.Sc, Jana Tomankova, Mgr. Karolína Svobodová and the rest of my colleagues who supported me with additional help and advice, and for their friendship during my master's degree. I would like to also thank Frederica Serati who started this interesting project and provided me all necessary information to continue.

Another thank you belongs to RNDr. Alena Bruce, Ph.D. for her kindness and willingness to provide me space for the laboratory work.

Finally, I thank my classmates/friends for their encouragement, friendship, and support during the whole period of studying. I am very delighted that I could spend these years with you, and we were able to pass all the challenges together.

Special thanks (in Slovak) – Najväčšie poďakovanie patrí mojej rodine, mojim úžasným rodičom za ich obrovskú podporu a pochopenie počas celého môjho štúdia. Mojej milovanej mamke za jej stále pozitívnu energiu a entuziazmus, ktorým ma dennodenne nabíja. Tatimu, za jeho rady, povzbudenia a stále dobre úmysly do mojej budúcnosti. Mojim dvom súrodencom, Erike a Janovi, ktorých mám neskutočne rada. Eri, tvoje povzbudivo-pravdivé slová ma stále nakopli.

Abstract

A complete understanding of preimplantation stages of mouse embryo development is still lacking. A technical mainstay of research into the specific function of individual genes/proteins during these stages has been the use of antibodies to detect expression and sub-cellular localisation using microscopic immuno-fluorescent staining approaches. However, this method is not 100% reliable, as antibodies are not always as specific as claimed and not all proteins have available and reliable anti-sera. Hence, one option to study specific proteins is to create transgenic embryos that incorporate genetically encoded fluorescence reporter proteins as fusions with endogenous candidate genes. Thus, permitting the expression level and subcellular localisation of specific genes to be assayed, across preimplantation developmental time, in both live and fixed embryos. We are adopting one such method to achieve this aim that exploits the CRISPR-Cas9 system to fluorescently tag candidate cell-fate related genes in mouse embryos. Thus, the main goal of my study was to create the necessary *in vitro* derived RNAs (*i.e.* specific guide RNAs/sgRNA and Cas9-Strepavidin mRNA) and biotinylated recombinant DNA repair template, required to edit endogenous candidate gene loci, by generating C-terminal mCherry fusions, in early embryonic cells. Such RNAs and dsDNA were co-microinjected into 2-cell stage mouse embryos, that were microscopically assayed for the expression and sub-cellular localisation of these candidate genes, revealed by fused mCherry fluorescent reporter tag, up until the peri-implantation blastocyst stages. To date, the optimisation associated with these constructs has resulted in detection of a potential *Mapk13*-mCherry fusion reporter gene and improvements to the experimental techniques are on-going in the laboratory (*i.e.* by my colleagues).

Key words: mouse preimplantation developmental stages, the first cell-fate decision, the second cell-fate decision, mCherry, WWC2, p38-Mapks, CRISPR-Cas9, fluorescent C-terminal tagging.

Table of contents

1. Introduction	2
1.1. Mouse Preimplantation Development.....	2
1.1.1. A brief overview of mouse preimplantation embryonic development.....	2
1.1.2. Oocyte development.....	3
1.1.3. Post fertilisation development.....	3
1.1.4. Embryonic robustness and clinical relevance.....	6
1.2. The first cell-fate decision (TE versus ICM).....	6
1.2.1. WWC2.....	10
1.3. Regulation of the second cell-fate in the murine blastocyst (PrE versus EPI).....	11
1.3.1. p38 mitogen-activated protein kinases (p38-MAPKs).....	12
1.4. Genome engineering with CRISPR-Cas9.....	13
2. Thesis project aims	18
3. Materials and Methods	19
3.1. Generation of biotinylated recombinant DNA repair templates for the microinjection.....	19
3.1.1. Preparation of gene specific homology arms (<i>Wwc2</i> , <i>Mapk13</i> and <i>Mapk14</i> genes) for cloning into pEasyFusion_mCherry plasmid.....	19
3.1.2. Cloning of gene specific 3' and 5' homology arms (<i>Wwc2</i> , <i>Mapk13</i> and <i>Mapk14</i>) into pEasyFusion_mCherry vector.....	22
3.1.3. Production of BIO-PCR dsDNA HDR template for CRISPR-Cas9 mediated genome editing (by homologous recombination).....	27
3.2. Gene specific single guide sgRNA production.....	29
3.2.1. Cloning of target gene-specific oligos (complementary to sgRNA) into pX330-U6-Chimeric_BB-CBh-hSpCas9 plasmid.....	29
3.2.2. Generation of sgRNAs by IVT.....	32
3.3. Generation of Cas9-streptavidin mRNA.....	34
3.4. Preimplantation mouse embryo specific methods.....	36

3.4.1. Preimplantation mouse embryo cultivation	36
3.4.2. Cytoplasmic microinjection of preimplantation 2-cell-stage mouse embryos	38
3.4.3. Embryo fixation and DAPI counter-staining	39
3.4.4. Confocal microscopy and image analysis.....	39
4. Results	40
4.1. Preparation of biotinylated recombinant DNA repair templates for <i>Wwc2</i> , <i>Mapk13</i> and <i>Mapk14</i> genes.....	40
4.1.1. Cloning of gene specific 3' and 5' homology arms (<i>i.e.</i> <i>Wwc2</i> , <i>Mapk13</i> and <i>Mapk14</i>) into pEasyFusion_mCherry vector.....	41
4.1.2. Production of target gene specific biotinylated dsDNA HDR templates	52
4.2. Generation of gene sequence specific sgRNAs (<i>Wwc2</i> , <i>Mapk13</i> and <i>Mapk14</i>)	55
4.2.1. Cloning of gene-specific oligos (<i>Mapk13</i> and <i>Mapk14</i>) into pX330-U6-Chimeric_BB-CBh-hSpCas9 plasmid	56
4.2.2. Generation of single guides RNAs (for <i>Wwc2</i> , <i>Mapk13</i> and <i>Mapk14</i>) prepared for the microinjection	58
4.3. Generation of Cas9-streptavidin mRNA	61
4.4. Assaying fluorescent mCherry-tagged endogenous gene expression (<i>i.e.</i> <i>Wwc2</i> , <i>Mapk13</i>) in peri-implantation mouse embryo blastomeres	63
5. Discussion.....	68
6. Conclusion.....	72
7. References	73
8. Appendix.....	80

Glossary of Abbreviations

adherens junctions	AJs
assisted reproductive technologies	ARTs,
bacterial-artificial-chromosome	BAC
bone morphogenetic protein	BMP
CRISPR Associated gene 9	CRISPR-Cas9
double-stranded DNA	dsDNA
double-strand breaks	DSB
embryonic stem cells	ESCs
epiblast	EPI
fibroblast growth factor-4	FGF4
guide RNA	gRNA
homology-directed repair	HDR
<i>in vitro</i> fertilisation	IVF
inner cell mass	ICM
meiosis I/II	MI/II
monomeric streptavidin	mSA
non-homologous end joining	NHEJ
p38 mitogen-activated protein kinases	p38-MAPKs
partitioning defective protein	PAR
polymerase chain reaction	PCR
primitive endoderm	PrE
protospacer adjacent motif	PAM
revolutions per minute	r.p.m
single guide RNA	sgRNA
super optimal broth with catabolite repression	SOC
TAL effector nucleases	TALENs
trans-activating crRNA	tracrRNA
trophectoderm	TE
ultraviolet	UV
zinc finger nuclease	ZFN
<i>zona pellucida</i>	ZP
zygotic genome activation	ZGA

1. Introduction

1.1. Mouse Preimplantation Development

1.1.1. A brief overview of mouse preimplantation embryonic development

The mouse is the most extensively studied model organism of mammalian preimplantation stage embryonic development; a period of robust, highly plastic and self-organising development (Tarkowski and Wroblewska, 1967). Mouse preimplantation embryonic development starts with the fusion of ovulated oocytes and sperm and extends over 4.5 days until the implantation of a fluid filled blastocyst stage embryo into the uterus wall. This process, initially comprises the transformation of the fertilized mouse egg into the totipotent zygote (note, totipotency in this context defines the ability of a cell to give rise to all embryonic and extraembryonic tissues needed to support full development to term) and is followed by several rounds of asynchronous cell cleavage divisions. The production of progressively smaller cells known as blastomeres, whose cytoplasmic volume does not exceed that of the initial zygote, leads to the emergence of a blastocyst comprising three distinct cell lineages. Two differentiating epithelia that eventually give rise to supportive extraembryonic tissues post-implantation (the outer trophoblast/TE and the superficial primitive endoderm/PrE lining the surface of an inner cell mass/ICM facing the fluid filled cavity) and the pluripotent epiblast (EPI – residing deep within the ICM) that serves as a progenitor pool for all cells of the subsequent foetus, Figure 1 (Chazaud and Yamanaka, 2016).

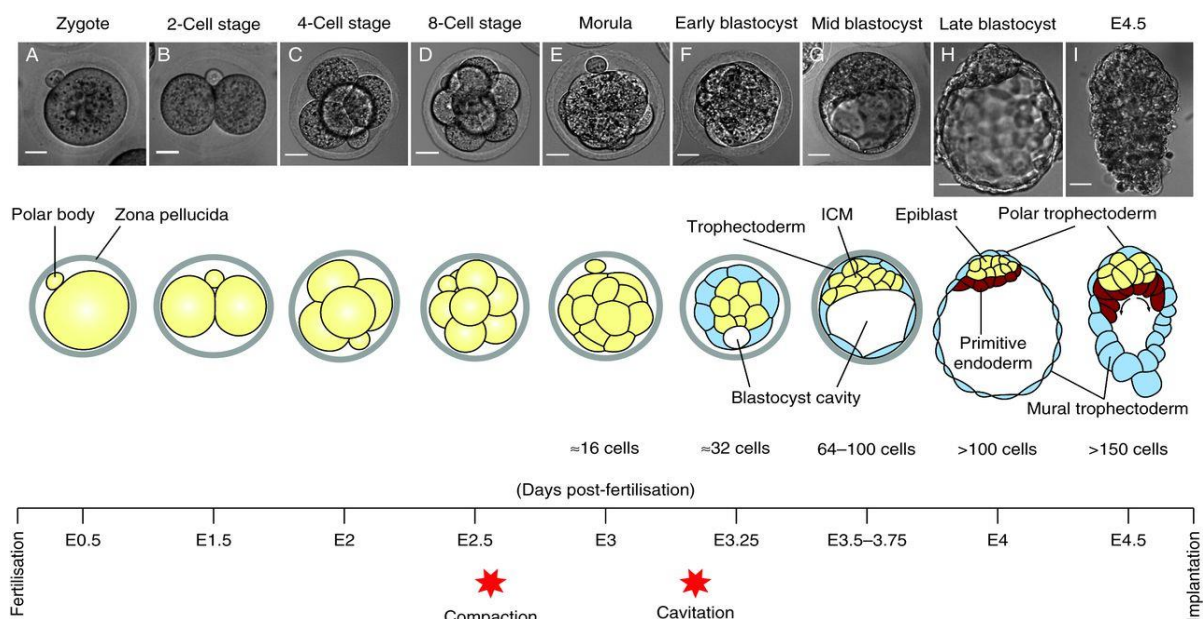


Figure 1. The preimplantation period of mouse embryo development; from the zygote to blastocyst stages. The fertilization of the meiotically matured oocyte initiates a developmental

process of asynchronous cleavage divisions that results in the formation of the pre-implantation stage blastocyst embryo, comprising three distinct cell lineages (trophectoderm, primitive endoderm and epiblast). The defining morphological events of embryo compaction and initiation of blastocyst cavity formation are highlighted, taken from Siaz and Plusa, 2013.

1.1.2. Oocyte development

Primary mouse oocytes (surrounded by a glycoprotein layer called the *zona pellucida* – ZP) are derived in the female ovary, prior to birth (Wassarman and Litscher, 2013), and are arrested in the prophase of meiosis I (MI) and are incompatible with fertilization. Under the periodic stimulation of maternal reproductive hormones, sub-populations of primary oocytes resume and complete MI (resulting in the formation of a vestigial polar body cell and the separation of homologous replicated chromosomes between oocyte and polar body) and immediately begin meiosis II (MII) shortly before, or during, their ovulation. However, such secondary oocytes arrest at the metaphase stage of MII, prior to fertilisation. The fertilisation of such arrested secondary oocyte by a single sperm (termed embryonic day zero – E0) in the oviduct, induces the completion MII (generating a second polar body and separating sister chromatids) and signals the formation of the totipotent zygote (comprising a balanced diploid complement of maternally and paternally inherited chromosomes) (Sanders and Jones, 2018).

As in other organisms, the early embryo developmental stages are initially dependent on messenger RNAs (mRNAs) and proteins maternally inherited from the egg (Schultz, 2002). Such maternal factors exclusively control and drive zygote development until the end of the 1-cell stage after which, the zygotic genome becomes transcriptionally activated (ZGA). The onset of ZGA is first initiated with a minor burst of transcription followed by a major burst at the end of the 2-cell stage. Subsequently, developmental processes are induced by major transcriptional activation of the embryonic genome. Accordingly, most of the maternal mRNA is degraded although proteins synthesised from maternal transcripts may persist during the whole pre-implantation development (Zernicka-Goetz *et al.*, 2009).

1.1.3. Post fertilisation development

The cell cycles of preimplantation blastomeres last around 12 hours, apart from the zygote and 2-cell stages (~6-8 hours longer) (Johnson, 2009; Brigid Hogan *et al.*, 1994). The entire process of mouse preimplantation is known to be under the control of an intrinsic, and as of yet, unidentified endogenous clock that dictates the developmental timing of distinct morphological events (*i.e.* embryo compaction, initiation of intra-cellular apical-basolateral

polarisation and blastocyst cavity formation – *further discussed below*). These events are important for the successful derivation of the three peri-implantation stage (E4.75) blastocyst cell lineages – TE, PrE and EPI (Figure 1) (Johnson, 2009). Evidence supporting the presence of the clock comes from experiments in which mechanically separate blastomeres of 2-cell stage embryos independently and constantly follow the same series of morphological transitions as intact control 2-cell embryos, despite consisting of half the number of cells (Morris *et al.*, 2012, Tarkowski, 1959).

Post-fertilisation, the first three rounds of cell cleavage give rise to 8-cell (E2.5) stage embryos in which the individual constituent blastomeres are spherical and morphologically distinct. However, by the late 8-cell stage, blastomeres begin to maximise their cell-cell contacts and the whole embryo compacts (making the definition of individual cells less obvious) into a structure known as the morula. Concomitant with compaction, late 8-cell blastomeres initiate intra-cellular polarisation along their radial axis, resulting in enrichment of specific complements of distinct polarity factors at the cell contactless apical, and contacted basolateral domains (Sutherland *et al.*, 1990).

The transition to the 16-cell (E3.0) stage morula is marked by two types of cell cleavage divisions that result in spatial segregation of daughter cells to either outwardly facing or inner/encapsulated positions (similarly repeated at the 16- to 32-cell stage transition, in the case of outer-residing cells). Such cleavage divisions are largely based on the orientation of the mitotic spindle and can be classified as *symmetric* (both daughter cells inherit part of the apical domain, hence remain polarised along their apical-basolateral axis, and remain located on the surface of the embryo) or *asymmetric* (whereby only one daughter cell inherits the apical domain, retains apical-basolateral polarity and remains on the outside, whereas the other, now apolar, cell is encapsulated to the inner embryo compartment) (Figure 2). Although spindle orientation may influence the extent of polarity daughter cells inherit, it is important to note that any apolar cells that initially occupy outer positions can actively sort to ultimately populate the nascent ICM. Additionally, in reality, not all divisions are perfectly symmetric/asymmetric and are most often oblique variations in which the relative degree of inherited polarity ultimately dictates their relative spatial location. Thus, by the 32-cell stage the embryo consists of polarised outer-cells that will form the TE and ultimately give rise to the embryonic component of the placenta (post-implantation) and an apolar ICM. This separation is often referred to as the first cell-fate decision (Chazaud and Yamanaka, 2016).

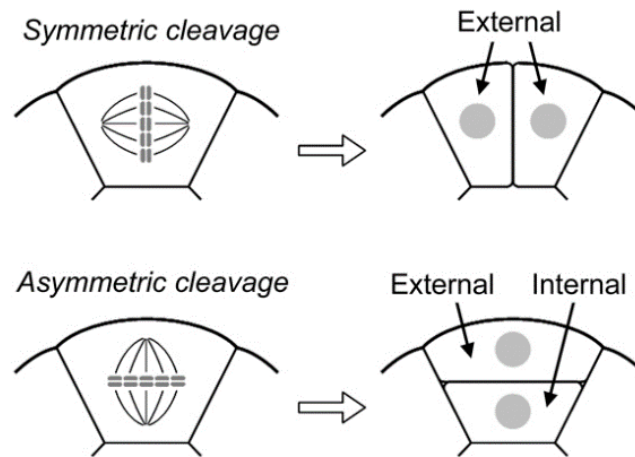


Figure 2. A schema showing the symmetric and asymmetric cell division in the mouse preimplantation stage. The symmetric cleavage results in two identical external cells whereas asymmetric division leads to generation of two different cells outside and inside the embryo. The apical domain contributes to orientating mitotic spindle along the apical basolateral axis (taken from Marikawa and Alarcón, 2009).

The 32-cell (E3.5) preimplantation embryonic stage is also characterised by the presence of an expanding fluid filled cavity that is the defining feature of the blastocyst. The blastocyst cavity is formed and expanded thanks to an osmotic gradient created across the TE, created by the action of Na⁺/K⁺ ATPase enzymes and water transport via transmembrane aquaporins (Eckert *et al.*, 2004). The expanding cavity displaces the ICM population of cells toward one pole of the blastocyst (termed the embryonic pole to distinguish it from the opposing abembryonic pole). The epithelial integrity of the TE maintains cavity expansion until the late blastocyst (E4.5) stage, at which point the embryo hatches from the glycoprotein ZP and completes uterine implantation. However, the hatching process is still not well described but the TE is considered to play a substantial role (White *et al.*, 2018). Concomitant with blastocyst cavity expansion, individual cells of the ICM either differentiate to form the PrE or specify themselves as EPI. A mechanism of active cell sorting is responsible for cells of each specified ICM cell lineage to occupy the distinct tissue layers observed by E4.5 (Figure 1). The PrE (that later develops into parietal and visceral endoderm and subsequently contributes to the yolk sac membranes) is arranged as a unicellular layer that separates the cavity from the deeper ICM layers of the EPI (the pluripotent cell lineage that gives rise to the embryo proper by producing all foetal cells). The segregation of EPI and PrE is commonly referred to as the second cell fate decision (Cockburn and Rossant, 2010; Chazaud and Yamanaka, 2016)

1.1.4. Embryonic robustness and clinical relevance

During preimplantation development, mouse (and mammalian) embryos are highly robust. This is demonstrated by their ability to develop readily and successfully in *in vitro* culture conditions. In synthetic and chemically defined culture media, mouse embryos are able to develop to the blastocyst stage and, after transfer back to the uterus, result in viable offspring. This an exceptional feature has been exploited in the development of assisted reproductive technologies (ARTs), especially *in vitro* fertilisation (IVF) (Goldberg *et al.*, 2007). Moreover, mouse (and mammalian) preimplantation embryo development is highly adaptable and can withstand major interventions caused by external forces. For example, if one 2-cell stage embryo blastomere is experimentally compromised, or each of the blastomeres are separated, development can continue to the blastocyst stage and to term (demonstrating totipotency of 2-cell stage blastomeres) (Tarkowski, 1959). Furthermore, the constituent blastomeres of preimplantation embryos can be disaggregated, rearranged or added to (using blastomeres or pluripotent cells of differing genetic origin, to form chimeric embryos) and still recapitulate a correct developmental programme resulting in appropriate blastocyst formation and full development of viable offspring (Tarkowski, 1961) (as has been exploited in generating transgenic animals by the incorporation of genetically modified embryonic stem cells/ ESCs). Such plastic and adaptable properties of preimplantation embryos are collectively referred to as *regulative* development and are distinct from the rigid and inflexible *deterministic* development of other non-mammalian species (*e.g.* *C. elegans* or *D. melanogaster*) that are unable to withstand such perturbations.

1.2. The first cell-fate decision (TE versus ICM)

(Hippo-signalling; polarity and cell positioning in preimplantation embryo lineage specification)

The first cell-fate decision takes place between the 8- to 16- and 16- to 32- cell transitions and leads to the spatial segregation of outer polarised blastomeres (that will contribute to the TE) from inner apolar nascent ICM cells (that ultimately yield both PrE and EPI lineages). Although the orientation of such cleavages and the subsequent spatial allocation of daughter cells is controlled by many complex processes (related to apical-basolateral polarisation), it is the specific expression of lineage restricted transcription factors that impart identity/fate to such segregated cells (Chazaud and Yamanaka, 2016; Saiz and Plusa, 2013).

The first lineage fate decision coincides with compaction and apical-basolateral polarisation of 8-cell stage blastomeres. 8-cell blastomeres individually retain a totipotent

capacity (being able to contribute to the TE, PrE and EPI lineages, when combined in chimeric embryos, but are not in isolation capable of sustaining full development), and are considered to be functionally equivalent (in terms of subsequent cell-fate) at this stage (Saiz and Plusa, 2013). The process of compaction involves the formation of adherens junctions (AJs) between neighbouring cells and is post-translationally regulated (as all protein components necessary for the initiation of compaction are already presented at the 4-cell stage) (Ducibella and Anderson, 1975). AJs not only mediate cell adhesion but also act as important sites of Hippo-signalling regulation, critical to establishing lineage specific transcription factor expression (*see below*). As 8-cell stage embryos compact, individual blastomeres also become intracellularly polarised, resulting in the asymmetric distribution of specific polarity factors to either the contactless apical domain (including PAR-aPKC and Crumbs protein complexes) or the opposing AJ enriched basolateral domains (containing the Scribble-PAR1/EMK1 complex) that remain in cell contact (Figure 3). (Iden and Collard, 2008; Hirate *et al.*, 2013; Hirate and Sasaki, 2015). The apical PAR (partitioning defective) protein complex, originally discovered in *C. elegans*, is active during mouse preimplantation development and comprises a class of three PAR homologs including as PAR3, PARD6b and aPKC (atypical protein kinase C) complexes. A fourth PAR protein, PAR1/EMK1, is dependent on cell contacts during compaction and thus, become distributed in the basolateral region (Vinot *et al.*, 2004, 2005). aPKC together with PAR3/Pard6b are initially localised in the contactless apical domain, with PAR3 ultimately becoming localised to tight junction regions that demark the apical and basolateral domains (Plusa *et al.*, 2005).

Indeed, the establishment of such apical-basolateral polarity is maintained by the formation/presence of tight-junction boundaries. The extent of apical polarity is known to impact the orientation of mitotic spindles (Korotkevich *et al.*, 2017), thus, influencing the degree to which ensuing divisions are symmetric/asymmetric (increased polarity favouring asymmetric divisions) and how apical-basolateral polarity is inherited (Figure 3). Furthermore, the degree to which apical-basolateral polarity is inherited between resulting daughter cells (both at the 16- and 32-cell stages) is central for both maintaining relative spatial position and initiating appropriate expression of lineage specific transcription factors (Davis and Tapon, 2019; Sasaki, 2017).

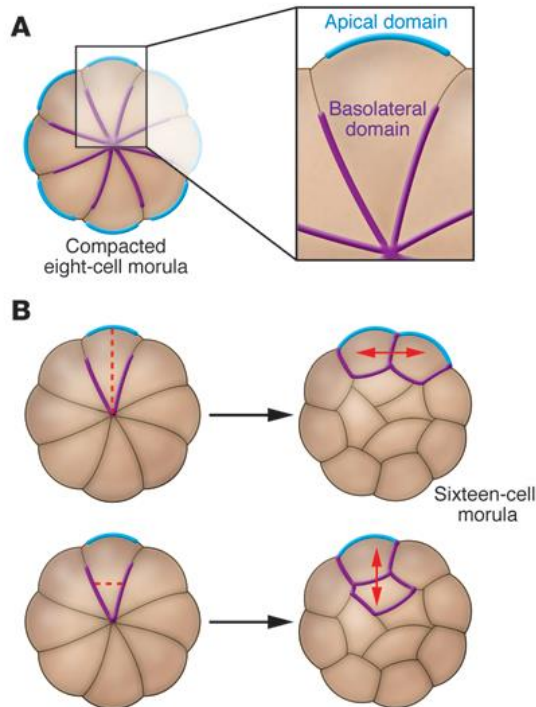


Figure 3. A schema of apical-basolateral polarity in the mouse preimplantation embryo.

(A) Establishment of the apical-basolateral membrane domains; an apical domain exposing outward, without contacts with other cells (blue) and a basolateral domain along membranes with cell-to-cell contact (purple). (B) Starting with the 8- to 16- cell transition, blastomeres are asymmetrically divided perpendicular to the inside-outside axis to produce one polar daughter cell (outside) and one apolar cell (inside), or blastomeres cleave symmetrically, in parallel to the inside-outside axis producing two polar cells (outside). These two types of cell division also occur as the embryo develops from 16- to 32- cells stage. Taken from Cockburn and Rossant, 2010.

The fate of spatially segregated and differentially polarised blastomeres (from the 16-cell stage onwards) is controlled by differential activation of the Hippo-signalling pathway (Sasaki, 2017) which was originally identified as a cell proliferation regulatory pathway in *D. melanogaster* (Davis and Tapon, 2019). In brief summary, the Hippo-signalling pathway is suppressed in apical-basolateral polarised outer cells to permit TE differentiation. Whereas, in apolar inner-cells, the active Hippo-signalling pathway inhibits TE differentiation and actively supports pluripotency (Sasaki, 2017). Specifically, the presence of the apical domain in polarised outer cells leads to the direct sequestration of the Hippo-signalling activator AMOT to the apical domain (Leung and Zernicka-Goetz, 2013). AMOT is therefore unable to localise at AJ localised Hippo-signalling centres, resulting in the failure to activate the pathway effector kinases LATS1/2. This in turn ensures the transcriptional coactivator YAP, a substrate of LATS, remains non-phosphorylated (Leung and Zernicka-Goetz, 2013, Hirate *et al.*, 2013) and is able to translocate to the nucleus and form a complex with the transcription factor TEAD4. This complex is directly responsible for activating transcription of the TE specific transcription factor gene, *Cdx2*, and initiates TE differentiation. Simultaneously, this process suppresses pluripotency related gene expression *e.g.* the transcription factor gene *Sox2*

(Nishioka *et al.*, 2008). Conversely, in apolar inner cells AMOT is free to associate with AJ localised Hippo-signalling centres, activates LATS1/2 and results in YAP phosphorylation. The phosphorylation of YAP blocks nuclear translocation and renders TEAD4 unable to activate TE specific gene expression. Moreover, active Hippo-signalling in inner cells actively promotes the expression of pluripotency related genes (*e.g. Sox2, Oct4/Pou5f1* and *Nanog*). Thus, the polarity dependent positioning of TE and ICM progenitor cells is reinforced by lineage appropriate gene expression under the regulation of polarity dependent differential Hippo-signalling (Figure 4) (Yagi *et al.*, 2007; Zhao *et al.*, 2007; Nishioka *et al.*, 2009; Sasaki, 2010).

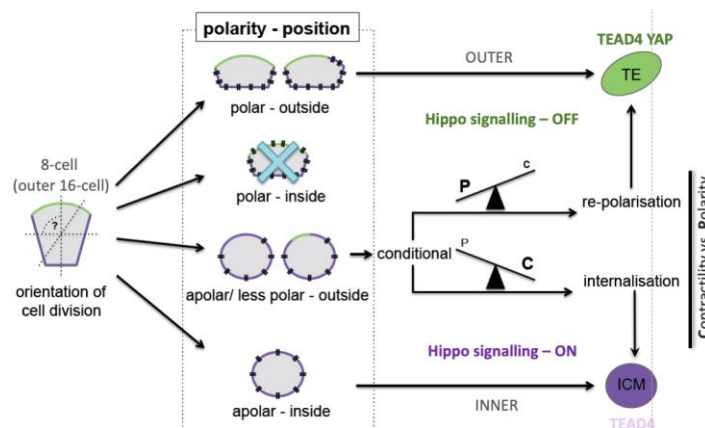


Figure 4. The relationship between polarity and cellular spatial position and Hippo-signalling pathway activation status in preimplantation mouse embryo. Hippo-signalling is inhibited in polarised outer cells, permitting YAP to enter the nucleus and form transcriptional complexes with TEAD4 to promote TE-specific gene expression (upper most scenario). Active Hippo-signalling, freed from polarity induced suppression, in apolar inner cells (lowest scenario) prevents TEAD4-YAP complex formation and associated TE-specific gene expression (and promotes pluripotent gene expression). The extent of derived daughter cell inherited polarity dictates ultimate spatial positioning in the embryo and the appropriate activity of the Hippo-pathway to specify the correct cell fate (central scenarios). Taken from Mihajlovic and Bruce, 2017).

As discussed above, the Hippo-signalling pathway was originally identified as a tissue growth and regulating pathway in *D. melanogaster* and is known to include many varied signalling inputs that regulate the activation status of the pathway's effector kinases (Davis and Tapon, 2019). One such component gene is *Kibra*, first described in *D. melanogaster* as a Hippo-pathway activator (Baumgartner *et al.*, 2010; Genevet *et al.*, 2010) and subsequently confirmed in the same role in mammals (Xiao *et al.*, 2011). Mammalian KIBRA belongs to a family of WW and C2 domain (WWC domain) containing proteins that comprises three

members (*i.e.* WWC1/KIBRA, WWC2 and WWC3, although the equivalent *Wwc3* gene has been specifically deleted from the *M. musculus* genome) and all three human derived proteins have been confirmed as positive regulators of the Hippo-signalling (Wennmann *et al.*, 2014). Given the central importance of Hippo-pathway regulation to the first cell-fate specification event of mouse preimplantation embryo development, our laboratory has been actively studying the potential functional role of WWC domain containing proteins during this period (Virnicchi *et al.*, 2020).

1.2.1. WWC2

WWC2 is a mammalian paralog of the Hippo-signalling activator WWC1/KIBRA, the human version of which has been confirmed mediate phosphorylation of the Hippo-pathway effector kinases LATS1/2 (Wennmann *et al.*, 2014). Compared to the extensive pan-model literature related to WWC1/KIBRA, relatively little is published about the functional role of any WWC2 proteins; limited to a few prognostic reports consistent with a tumour suppressor role in certain specific cancers (Zhang *et al.*, 2017; Han *et al.*, 2018). However, recently published data from our laboratory has shown that *Wwc2* gene has a key role in the acentrosomal cell divisions of mouse oocyte meiosis and early preimplantation mouse embryo cleavage divisions (Virnicchi *et al.*, 2020). Briefly, the uncovered phenotypes associated with specific RNAi mediated knockdown of *Wwc2* expression reveal defects in forming the meiotic spindle and subsequent segregation of homologous chromosomes during MI (that involve a failure to activate the crucial cell division regulatory kinase Aurora-A/AURKA - reviewed in Nguyen and Schindler, 2017). They also included impaired cell proliferation and defective mitotic cell divisions in preimplantation mouse embryos (evidenced by abnormal nuclear morphology and multiple micronuclei, indicative of aberrant chromosome segregation) and biased cell fate contribution of *Wwc2* knockdown cell clones against the pluripotent EPI blastocyst lineage (suggesting Hippo-signalling pathway activation defects) (Virnicchi *et al.*, 2020). Although we have uncovered an important role for WWC2 in early mouse embryo development, it has not proven possible to visualise the sub-cellular localisation of the WWC2 protein in this context, as sufficient quality anti-sera do not exist to perform immunofluorescent confocal microscopy analysis. Therefore, we decided herein to select the *Wwc2* gene for potential preimplantation mouse embryo CRISPR-Cas9 mediated gene editing, in order to create an endogenous WWC2-fluorescent reporter system.

1.3. Regulation of the second cell-fate in the murine blastocyst (PrE versus EPI)

After the execution of the first cell-fate decision (whereby the 32-cell (E3.5) stage blastocyst has segregated the specified outer TE lineage and the ICM), the second cell fate decision is initiated within the ICM and results in the emergence of the PrE and EPI lineages, by the late blastocyst (E4.5) stage. The PrE comprises a monolayer of cells along the ICM surface that faces the cavity (and is a progenitor pool of the extraembryonic yolk sac membranes) whilst the EPI is resident in the deep ICM and serves as a source of all future embryo/foetal cells (Cockburn and Rossant, 2010).

At the early blastocyst stage (E3.25), all ICM cells are unspecified with regard to future PrE or EPI cell-fate and co-express both NANOG and GATA6 transcription factor proteins (markers that by the late blastocyst (E4.5) specifically delineate the EPI and PrE lineages, respectively). However, as development proceeds this pan-ICM population of NANOG and GATA6 co-expressing cells resolves to a point (~E3.75-E4.0) in which the majority of cells have downregulated one or other of the markers. This mutually exclusive pattern of either NANOG or GATA6 expressing ICM cells is randomly distributed throughout the ICM and is referred to as the ‘salt & pepper’ pattern (Chazaud *et al.*, 2006) and reflects cells that will ultimately contribute to the pluripotent EPI or differentiating PrE, respectively. In the developmental time between the emergence of the salt & pepper pattern and the late blastocyst (E4.5) stage, the specified EPI and PrE progenitors actively sort into the two characteristic tissue layers, or if unable to migrate appropriately initiate apoptosis (Plusa *et al.*, 2008). As the two ICM lineages emerge, their identity is reinforced by specific expression of cell fate markers. For example, NANOG positive EPI cells also express the pluripotency marker SOX2, whereas differentiating PrE cells sequentially activate the expression of the transcription factors SOX17 and GATA4. The extent to which specification and emergence of the two ICM lineages is a stochastic process or is influenced by previous ancestor cell history (*e.g.* whether the nascent ICM cell was generated in the 8- to 16- or 16- to 32-cell transition) is a subject of debate (Chazaud and Yamanaka, 2016; Chazaud *et al.* 2006; Morris *et al.*, 2010; Krupa *et al.*, 2014). Interestingly, both EPI and PrE progenitors express the transcription factor OCT4 (POU5F1) and it has been shown that OCT4 forms a functional transcription complex with SOX2 in the emerging EPI and SOX17 in the differentiating PrE (Aksoy *et al.*, 2013).

As stated above, NANOG is an epiblast marker but is nevertheless required for formation of the PrE. This is exemplified by the fact that initiated PrE differentiation cannot continue (as assayed by sequential expression of SOX17 and GATA4) in the absence of the *Nanog* gene (Frankenberg *et al.*, 2011). However, this defect can be rescued by the exogenous addition of Fibroblast growth factor-4 (FGF4), one of the earliest up-regulated genes in specifying EPI cells (Guo *et al.*, 2010; Ohnishi *et al.*, 2014). In fact, active FGF4 signalling, particularly in the context of downstream activation of the ERK1/2 pathway, plays a central role in specifying and driving PrE differentiation (Yamanaka *et al.*, 2010; Nichols *et al.*, 2009). This is largely achieved by a gradual specification of PrE from an ever-reducing pool of uncommitted ICM cells, that thus maintains the final balance of EPI and PrE by the late blastocyst (E4.5) stage (Siaz *et al.*, 2016). Additionally, PrE differentiation can also be positively influenced by the action of Bone morphogenetic protein (BMP) signalling (Chazaud and Yamanaka, 2016). It was also recently demonstrated that p38 mitogen-activated-kinases (p38-MAPKs that belong to the same super-family of serine-threonine and tyrosine kinases as ERK1/2) can also regulate the emergence of EPI and PrE during the second cell-fate decision (Thamodaran and Bruce, 2016).

1.3.1. p38 mitogen-activated protein kinases (p38-MAPKs)

The p38-MAPKs are a class of four paralogous mammalian proteins expressed during preimplantation mouse embryo development (comprising p38 α – expressed from the *Mapk14* gene, p38 β /*Mapk11*, p38 γ /*Mapk12*, p38 δ /*Mapk13*). All four *p38-Mapk* transcripts are expressed to varying degrees during preimplantation mouse embryo development. *Mapk14* and *Mapk13* transcripts represent the highest levels of steady expression throughout the period and contrast with levels of *Mapk11* mRNA that exists at basal levels of expression. The initially lower expression of *Mapk12* transcripts is known to gradually increase to levels equivalent to those observed for *Mapk13/14* by the late blastocyst (E4.5) stage (Natale *et al.*, 2004). Although, p38-MAPKs belong to the wider super-family of serine-threonine and tyrosine mitogen activated kinases (Cargnello and Roux, 2011), they are not classically known to be activated by liganded growth-factor associated receptor tyrosine kinases. Indeed, they are most characterised as being activated by extracellular stimuli, such as pro-inflammatory cytokines, UV radiation and physical/mechanical stress (Remy *et al.*, 2010). Activated p38-MAPKs are predicted to phosphorylate and regulate between 200 and 300 cellular substrates, including transcription factors, chromatin remodellers or other kinases (Cuadrado and

Nebreda, 2010). Published reports from our own laboratory have uncovered a role for active p38-MAPK during the early stages of blastocyst ICM cell fate specification (using a pharmacological inhibition mediated experimental approach). Specifically, that p38-MAPK activity enables the initially uncommitted ICM cells, co-expressing NANOG and GATA6, to specify and differentiate towards the PrE lineage, in a mechanism that appears to be downstream of active FGF-receptor tyrosine kinase signalling (Thamodaran and Bruce, 2016; Bora *et al.*, 2019). We propose that p38-MAPK(s), potentially under the control of active FGF4 signalling, prime the PrE progenitor cells of the ICM for subsequent PrE differentiation, that is then driven to completion by activated ERK1/2 signalling (*manuscript in preparation*). It is for these reasons that we selected two p38-*Mapk* genes (*Mapk13* & *Mapk14* – as our most promising candidates to mediate the second cell fate decision phenotypes which we observed after p38-MAPK inhibition) for potential CRISPR-Cas9 mediated addition of fluorescent reporter tags in preimplantation mouse embryos (as it is also described for *Wwc2*).

1.4. Genome engineering with CRISPR-Cas9

Since the discovery of the DNA double helical structure, there have been many technologies developed that aim to manipulate and synthesise custom DNA sequences. It ranges from *in vitro* recombinant DNA based approaches to *in vivo* genome editing techniques, including bacterial-artificial-chromosome (BAC) recombineering or more direct site-directed zinc finger nuclease (ZFNs) or TAL effector nucleases (TALENs) genome editing. Despite the development of these latter *in vivo* editing techniques, there still remain significant barriers to their widespread and routine adoption, mostly due to of difficulties of required protein design or synthesis (Kim *et al.*, 1996; Christian *et al.*, 2010). However, the recently developed CRISPR-Cas9 system has emerged as an affordable and relatively convenient way to precisely edit living cell genomes of animals and plants, *in situ* (Doudna and Charpentier, 2014). CRISPR is an acronym for the Clustered Regularly Interspaced Short Palindromic Repeats sequences, originally identified in the genome of *Escherichia coli* (but now identified in many bacterial and archaea species). They are defined as a series (termed an array) of unique targeting sequences that are interspaced with short identical sequence repeats. The unique targeting sequences are derived from bacterial specific viruses and have been incorporated into the host bacterium's CRISPR array as a record of past infection and are mobilised in an adaptive bacterial immune response to subsequent infection by the same viral type (Ishino *et al.*, 1987; Mojica *et al.*, 2000). The bacterial CRISPR genetic loci also encodes a series of *cas*

(CRISPR-associated) genes, organized in operons, that encode proteins with nuclease and helicase activity (Haft *et al.*, 2005). Hence, processed RNA transcripts from the CRISPR arrays, called crRNAs (note, such processing is controlled by a subset of *cas* encoded proteins), are able to complex with specific *cas* encoded proteins and are targeted to invading/foreign nucleic acid sequences (such as those resulting from viral infection) by means of base-pair complementarity to catalyse their destruction (Makarova *et al.*, 2006; Brouns *et al.*, 2008). There are three main described alternatives of the CRISPR/Cas system, that each use distinct molecular mechanisms to achieve nucleic acid recognition and cleavage (Makarova *et al.*, 2011). However, from here on this thesis will focus on the CRISPR-Cas9 variant that belongs to the Type II classification and only requires a single protein (*i.e.* Cas9) to catalyse RNA-guided DNA recognition and cleavage (Gasiunas *et al.*, 2012).

The multifunctional Cas9 protein consists of two nuclease domains, a HNH domain (required to cleave the target dsDNA strand that is complementary to the 20-nucleotide sequence of crRNA) and a RuvC-like domain (needed to cleave the DNA strand opposite the complementary strand) (Gasiunas *et al.*, 2012). The characterised CRISPR-Cas9 protein complex from *Streptococcus pyrogenes* is known as a dual-RNA-guided DNA endonuclease. This is because in addition to crRNA, DNA sequence specific targeting of the Cas9 protein also relies a second trans-activating crRNA (tracrRNA). tracrRNA is partially complementary to the repeat portion of the crRNA and hybridises with it and only this hybrid crRNA-tracrRNA can guide the Cas9 protein to its target DNA sequence (Figure 5 – *left*). As the CRISPR-Cas9 system has been adapted for specific experimental genome editing (in non-bacterial species – *as described below*), the use of crRNA-tracrRNA hybrids has been superseded by the development of single guide RNAs (sgRNAs) that combine the functions of both components into one RNA molecule (via the incorporation of a loop between the 3' end of the crRNA and 5' end of the tracrRNA (Figure 5 – *right*)) (Deltcheva *et al.*, 2011). As such functional sgRNAs must consist of a 20-nucleotide sequence at the 5' end that determines specificity to the targeted DNA site, and an intra-molecular double stranded structure at the 3' portion that binds the Cas9 protein (Jinek *et al.*, 2012). The specificity of target DNA recognition by the Cas9 complex is not solely determined by complementarity with the crRNA component, but also it is determined by a short sequence known as the protospacer adjacent motif (PAM) which must be present in an adjacent region of the targeted sequence (Jinek *et al.*, 2012; Gasiunas *et al.*, 2012). PAM motifs in the Type II CRISPR-Cas9 systems consist of

a NGG consensus sequence (*i.e.* comprising two G:C base pairs on the non-complementary strand of the target DNA, one base pair downstream of the crRNA binding sequence). The main role of the PAM sequence is to direct the Cas9 complex, together with crRNA-tracrRNA/sgRNA to the correct target DNA site (Jinek *et al.*, 2012). The PAM is also critical for initial DNA binding, as in its absence the Cas9 complex is not able to bind DNA despite the fully complementary sequences of the crRNA/sgRNA and the targeted DNA (Anders *et al.*, 2014; Sternberg *et al.*, 2014).

Since the description of the natural role of the Type-II CRISPR-Cas9 system in bacterial innate immunity, the system has been optimised to specifically target sequence defined genomic loci in living cell nuclei of many other species. Thus, there has been created a simple two-component system (Cas9 as a DNA endonuclease guided by sgRNA) to target and cleave any *in situ* DNA sequence of interest (Jinek *et al.*, 2012; Doudna and Charpentier, 2014).

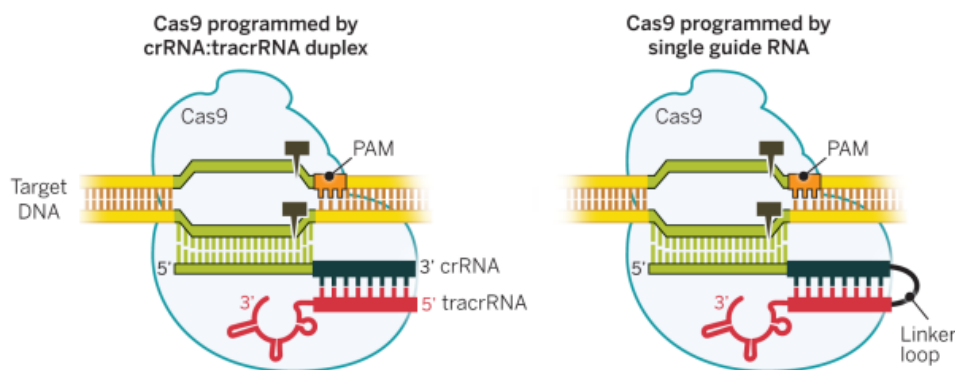


Figure 5. The structure and differences of Cas9 complex associated with crRNA:tracrRNA duplex (left) versus single guide RNA containing linker loop (right), taken from Doudna and Charpentier, 2014.

Thus, the optimised CRISPR-Cas9 system enables efficient *in situ* genome editing in living cells and can be employed to knock-out or knock-in specific heterologous DNA sequences at sequence defined genomic loci. Accordingly, the DNA double-strand breaks (DSB) made at the specific genomic loci by the custom designed RNA-guided Cas9 complex are repaired by endogenous cellular DNA repair mechanisms. It is either via the non-homologous end joining DNA repair pathway (NHEJ) or homology-directed repair (HDR) pathway (Figure 6). Non-homologous end joining (NHEJ) is a prevalent but error prone

mechanism of DNA double strand break repair that introduces site specific insertions/deletions (indels) at the break point. Therefore, NHEJ repair effectively and functionally disrupts a targeted gene's activity (*e.g.* disrupting a gene promoter to prevent transcriptional initiation or by the generation exonic frame shift mutations that lead to the generation of nonsense coded mRNA transcripts). In essence, it generates gene knockout/loss of function alleles (Figure 6 – *left*). Conversely, the HDR DNA repair pathway requires a double stranded DNA sequence that is homologous across the region of the DNA double stranded break, that then acts as template for the faithful repair (at the single nucleotide level) of the damaged DNA (in diploid cells this is usually provided by the homologous chromosome). Consequently, no indels are created around the original site of the double stranded DNA break. However, in the context of CRISPR-Cas9 mediated gene editing, the HDR pathway can be experimentally exploited to introduce foreign DNA sequences at define loci (*i.e.* to create genetic knock-ins, *e.g.* to add in frame cDNA sequences for fluorescent reporter proteins to specific gene loci, thus generating tagged fusion proteins under the genetic control of the endogenous locus – as is the aim of the experiments described in this thesis). Such knock-ins require the generation of a HDR double stranded DNA template that comprises the intended foreign DNA sequence to be inserted, flanked by a substantial region of sequence homology to the genomic loci to be targeted (*i.e.* either side of the indented double stranded DNA break point). This template is then provided with the sgRNA and Cas9 and is used by the cells endogenous HDR apparatus to repair CRISPR-Cas9 introduced double strand break and hence faithfully introduces the foreign DNA into the genome (Figure 6 – *right*) (Hsu *et al.*, 2014).

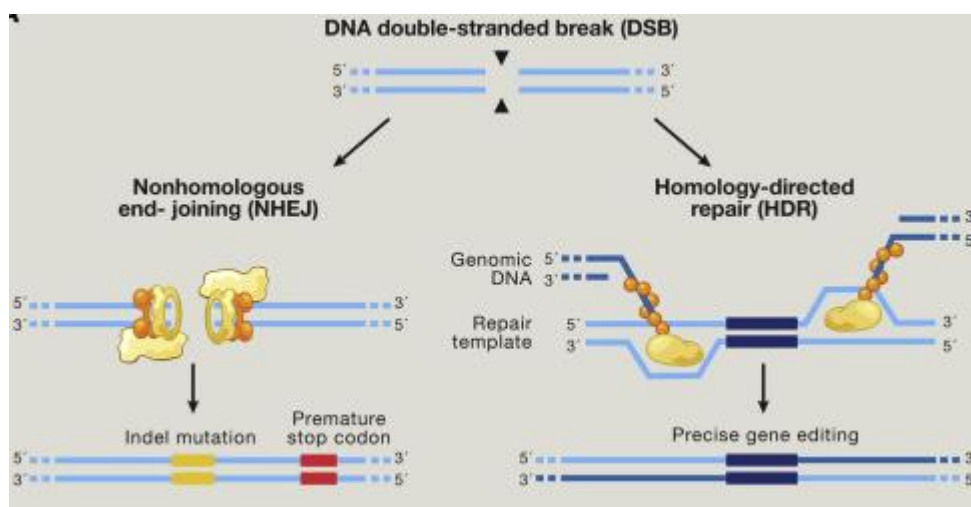


Figure 6. The mechanism(s) of CRISPR-Cas9 mediated genome editing (taken from Hsu *et al.*, 2014). A single guide RNA, specific to the DNA target interacts with Cas9 protein (with endonuclease activity) resulting in a RNA-guide-Cas9 complex. The complex recognizes the DNA region of interest, binds and causes target-specific double-stranded DNA cleavage (DSB - *top*). The cleavage site can be repaired by the non-homologous end joining (NHEJ - *left*) DNA repair pathway or homology-directed repair (HDR - *right*) pathway which is based on homologous recombination and requires the presence of a homologous double stranded DNA repair template (Hsu *et al.*, 2014).

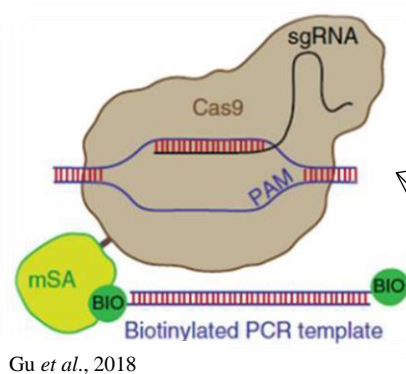
There are many reported studies employing the CRISPR-Cas9 technique to *in situ* edit the genomes of living human and mouse cells (Cong *et al.*, 2013; Jinek *et al.*, 2013). Recently, this revolutionary method has been optimised to edit the genomes of mouse zygotes and 2-cell stage embryos (Gu *et al.*, 2018). In this research, the authors describe the targeted knock-in of fluorescent cDNA sequences in place of the stop codons of several endogenous mouse genes, thus editing endogenous genes to encode C-terminal fluorescent fusion proteins (mainly mCherry) that could be visualised in live and fixed preimplantation embryos. Specifically, to generate useful transgenic reporter mouse strains after transfer of edited embryos, at the early blastocyst/E3.5 stage, to the uteruses of pseudo-pregnant foster mother mice. The authors report the highest levels of editing efficiency were obtained by microinjecting the required reagents (*i.e.* sgRNA, Cas9 mRNA and HDR-mCherry double stranded DNA template) into 2-cell stage blastomeres during the late S-G2 phase of the cell cycle (as measured by the expression of fluorescent-fusion proteins of known late blastocyst/E4.5 stage lineage makers, *e.g.* *Cdx2* in TE, *Nanog* in EPI and *Gata4* in PrE). Thus, permitting the visualisation and live imaging of the molecular and cellular dynamics of the targeted proteins during the preimplantation developmental process (Gu *et al.*, 2018).

2. Thesis project aims:

- Construction of CRISPR-Cas9 reagents and recombinant DNA constructs associated with the aim of creating C-terminal mCherry (fluorescent reporter) fusions for endogenous genes (*i.e.* *Wwc2*, *Mapk13*, *Mapk14*) in mouse preimplantation embryos.
- Characterization of fusion gene expression and localization, post-genome editing, during preimplantation mouse embryo development (*i.e.* after individual blastomere CRISPR-Cas9 reagent microinjection at the late 2-cell stage) using confocal microscopy.

The experimental project flow diagram summary:

- ★ Derivation of CRISPR-Cas9 complex required target gene/ genome editing reagents.



Recombinant DNA repair template (dsDNA HDR)

- Cloning target gene specific homology arms in pEasyFusion mCherry plasmid
- Derivation of BIO-PCR biotinylated dsDNA HDR templates

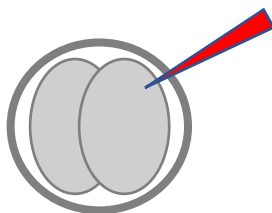
Target gene specific sgRNA (around STOP codon)

- Cloning gRNA into pX330-U6 plasmid
- Creating T7 RNA polymerase *in vitro* transcription (IVT) template by PCR
- IVT to derive sgRNA

Cas9-streptavidin mRNA

- IVT of Cas9-mSA mRNA from pCS2-Cas9-mSA plasmid

- ★ CRISPR-Cas9 reagent microinjection into one blastomere of 2-cell stage embryos.



- ★ Characterisation of target gene-mCherry fusion gene protein expression and localisation by confocal microscopy at later embryonic stage. Assessment of

3. Materials and Methods

The construction of the required CRISPR-Cas9 reagents was started by a previous ERASMUS student, Federica Serati, during her traineeship in our laboratory (2019), after which I took over the project.

3.1. Generation of biotinylated recombinant DNA repair templates for the microinjection

3.1.1. Preparation of gene specific homology arms (*Wwc2*, *Mapk13* and *Mapk14* genes) for cloning into pEasyFusion_mCherry plasmid

For each targeted gene (*i.e.* *Wwc2*, *Mapk13* and *Mapk14*), two specific homology arms were produced by standard PCR comprising ~1.2 kb dsDNA fragments with sequence identity from each side of the endogenous gene STOP codon (*i.e.* the 5' arm and the 3' arm). Such PCR products were cloned in-frame either upstream or downstream, respectively, of the mCherry coding sequence of the pEasyFusion_mCherry plasmid – obtained from Addgene, clone number: 112849, see appendix for plasmid map, Figure 33. Such recombinant plasmid acted as template for the generation of biotinylated dsDNA HDR template to be microinjected into individual mouse embryo blastomeres. Hence, the PCR primers used to amplify the 5' and 3' homology arms incorporated necessary restriction enzyme sequences (specific to each targeted gene, see Table I) to facilitate cloning either upstream or downstream of the mCherry sequence of pEasyFusion_mCherry. Thus, the total reaction volume, per targeted gene homology arm, was 50µl; containing 25µl of 2X High Fidelity Phusion DNA Polymerase Master-Mix (New England BioLabs), 2.5µl DMSO (dimethyl sulfoxide, note for the 5' arm of *Mapk14* gene, it was necessary to use 4µl of DMSO), 200ng of genomic DNA (gDNA – previously isolated in the laboratory from mouse tail tissue), 2.5 µl of each sense/antisense gene-specific primers (the concentration 10µM). The PCR programme cycle was performed, in conventional PCR machine, as shown in Table II. To derive the most efficient primer annealing temperatures for the generation of each targeted gene homology arm, gradient PCRs had been previously employed using conventional 2X DreamTaqTM Green PCR Master Mix (Thermo Scientific). Specific primer annealing temperatures, with elongation time (based on the product size) and are detailed in Table III. The correct size of the generated PCR products (using 2X High Fidelity Phusion DNA Polymerase Master-Mix and Taq DNA polymerase) were confirmed by 1% agarose, ethidium bromide-stained, gel electrophoresis in 1X TAE buffer (*i.e.* 100-

150ng of PCR reaction was mixed with the 6X DNA-loading dye/water (New England BioLabs) and subsequently loaded into one well of the gel, alongside a lane loaded with 2µl 1KB+ marker ladder (Thermo Scientific).

Table I: Primers and their composition used for PCR reaction. (5' S/A) 5' homology arm sense/antisense, (3' S/A) 3' homology arm sense/antisense.

Target sequence: <i>Wwc2</i>		
Primer	Sequence	Restriction digest/site
5' S	GACTATgatattCCCACCTATCCTGACGTGGTGGC	<i>EcoRV</i>
5' A	ATAGTCgatattCACGTCGTCAGCGGGCAG	
3' S	GACTATggatccTGAACCTGCCTGTGGCTTAGCAC	<i>BamHI</i>
3' A	ATAGTCggatccGTCAAGCTTGCTTGTTCATCCAGA	
Target sequence: <i>Mapk13</i>		
Primer	Sequence	Restriction digest/site
5' S	GACTATgaattcTGGAGCCAGGAGTGTCTGCCAG	<i>EcoRI</i>
5' A	ATAGTCgaattcCTGCAGCTTCATGCCACTTCGT	
3' S	GACTATggatccTGAATTGATGGCTGGCCTCCATGTAGC	<i>BamHI</i>
3' A	ATAGTCggatccCTCCTGCCATTACCAGCGTGC	
Target sequence: <i>Mapk14</i>		
Primer	Sequence	Restriction digest/site
5' S	GACTATgaattcGTCCAGGGCAGGCTAGCGTG	<i>EcoRI</i>
5' A	ATAGTCgaattcGGACTCCATTTCTTCTTGGTCAAGGGG	
3' S	GACTATggatccTGAACACCTGGTTTCTGTTCTGTCTATCTCAC	<i>BamHI</i>
3' A	ATAGTCggatccGAGAGGACTCGTTTTCTGAATTGGTG	

The PCR primers used to generate the gene specific 5' and 3' homology arms were designed in advance by my supervisor doc. Bruce. As referenced above, in addition to the target gDNA complementary region, each primer includes an extra sequence to incorporate an appropriate restriction site (plus a six nucleotide spacer – to aid restriction enzyme digestion) at its 5' end, for cloning into the pEasyFusion_mCherry vector. Each PCR product was designed to be ~1.2Kb in length (thus aiding the ultimate efficient *in situ* genome editing incorporation of the mCherry coding sequence containing dsDNA HDR template into the microinjected mouse embryo blastomere genome, after the target region is nicked by Cas9). For each of the three targeted genes, the 3' homology arm contained a STOP codon, that when cloned into pEasyFusion_mCherry would be located just downstream, and in frame with, the mCherry coding sequence. Ensuring that post genome editing, the target gene-mCherry fusion RNA would only be translated as far as the end of the mCherry coding sequence (but would

be associated with the endogenous target gene 3' UTR). Note, all primers were sourced as desalted and lyophilized preparations from the Sigma Aldrich company.

Table II: PCR program used for the amplification of individual homology arm. *The temperature during annealing step depends on the melting temperature TM of specific gene. ** The time of elongation cycle hinges on the length of the PCR product.

PCR program	Temperature	Time
denaturation	98°C	2'
denaturation	98°C	30''
annealing	62-68°C *	30''
elongation	72°C	1'-2' **
extension	72°C	10'
cooling	4°C	∞

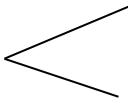
38x 

Table III: Primer annealing temperatures for the generation of each targeted gene homology arm (5' and 3'), their product sizes and elongation time. (AT) annealing temperature, (ET) elongation time.

Gene name	Homology arm	AT	The product size	ET
<i>Wwc2</i>	5'	63°C	1262bp	1' 30''
<i>Mapk13</i>	3'	62°C	1073bp	1' 30''
	5'	68°C	1158bp	1' 30''
<i>Mapk14</i>	3'	62°C	1137bp	1' 30''
	5'	62°C	1258bp	1' 30''

Judging by the appearance of the derived PCR products on resolved 1% agarose gels, they were either immediately purified using QIAquick PCR purification kit (Qiagen) or if more than one band was observed, that corresponding to the correct anticipated size was gel extracted (GenEluteTM Gel Extraction Kit, Sigma) according to the kit manufacturer's protocol. The now purified gene-specific and amplified homology arms were quantified by UV spectrophotometry (Nanodrop) and used as template in restriction enzyme digests, with gene appropriate restriction enzymes (*i.e.* corresponding to those recognition sequences introduced into the 5' portions of the PCR products by the oligonucleotide primers used - see Table I). The restriction enzyme digested reaction volumes used were 50µl, incubated at 37°C overnight and subsequently purified using the PCR purification Kit (QIAQuick) according to the manufactured protocols. The exact composition of each restriction enzyme digestion is

displayed in Table IV. The concentration of the resulting purified PCR products (*i.e.* gene-specific homology arms) containing sticky/cohesive ends compatible for cloning, was again measured by UV-spectrophotometry (Nanodrop).

Table IV: The reaction composition of the restriction enzyme digestion. * PCR product (homology arms) was used as template. The same conditions were used later for EasyFusion mCherry plasmid digestion.

Reagent	Volume
Cut Buffer (10X)	5 μ l
Template*	2 μ g
Restriction enzyme	1 μ l
HPLC water	up to 50 μ l
Total volume	50μl

3.1.2. Cloning of gene specific 3' and 5' homology arms (*Wwc2*, *Mapk13* and *Mapk14*) into pEasyFusion_mCherry vector

The pEasyFusion_mCherry vector (that already contains a cloned cDNA for the mCherry fluorescent protein (see appendix for plasmid map, Figure 33) was digested with a specific restriction enzyme (depending upon the gene specific homology arm to be cloned). Because each of the three targeted genes 3'-homology arms (identical to the region of the genomic sequence downstream of the STOP codon) were designed to be incorporated into pEasyFusion_mCherry using the restriction enzyme *BamHI* (see PCR oligo primer Table I), the plasmid was first digested with this enzyme. The appropriate restriction sites and composition of restriction enzyme digestion reactions of pEasyFusion_mCherry are displayed above, in Table I and IV. To prevent self-ligation of the linearized vectors (*i.e.* without incorporating the intended insert) the phosphates at the exposed terminal ends of the linearized plasmid were immediately, after digestion, removed by treatment with 1-2 units of alkaline phosphate (Roche Diagnostics GmbH, Germany) according to manufacturer protocol (see Table V for reaction composition). The resulting digested and treated vector was then purified by a conventional phenol-chloroform organic extraction, as follows: The overall sample volume of 50 μ l was increased to 300 μ l by addition of 250 μ l of HPLC water and an equal volume of 10mM Tris saturated phenol-chloroform (*i.e.* pH 8.0, for DNA extraction) was added, vigorously mixed (*i.e.* vortexed) and spun in a bench top microfuge for five minutes at 16 000 r.p.m. The upper aqueous phase, containing DNA, was carefully transferred into a new 1.5ml Eppendorf tube, to which an equal volume of chloroform, around 250 μ l, was added,

vigorously mixed and again centrifuged for five minutes at 16 000 r.p.m (to remove traces of phenol). The upper phase was again transferred to a new 1.5ml Eppendorf and mixed with a 1/10 volume of pH 5.2 3M NaAc (sodium acetate salt solution), 600µl of 100% ethanol and 2µl of glycogen (5mg/ml), vigorously mixed and left to precipitate overnight at -20°C. The sample was then centrifuged for 35 minutes in a pre-cooled (4°C) microfuge at 16 000 r.p.m. and the supernatant removed from the resultant DNA/glycogen pellet. The pellet was washed twice with 600µl of 70% ethanol for 15 minutes, centrifuged at 4°C at 16 000 r.p.m (to back extract the NaAc salt). The supernatant was again carefully removed, and pellet dried to the air. The dried pellet size, was typically resuspended in ~25µl adequate HPLC water/nuclease free water and the concentration and purity of DNA was measured by UV spectrophotometry (Nanodrop). To confirm plasmid linearization the digested plasmid was electrophoresed alongside the same amount of uncut vector. After such vector linearization, purification and gel electrophoresis verification (plus the derivation and purification of compatible restriction enzyme digested 5' or 3' gene specific homology arm PCR products which are described in the section 3.1.1), two components were ligated in a typical reaction mixture, as described in Table VI. The required molar quantities of prepared insert and vector (5:1 ratio, respectively) were calculated using the available online NEBio calculator tool (<https://nebiocalculator.neb.com/#!/ligation>). The ligation reaction consisting of vector and insert, plus a negative control (*i.e.* were HPLC water was added instead of insert – to assay the frequency of vector relegation without the incorporation of insert, *i.e.* background ligation) was incubated for 20 minutes at room temperature, then overnight at 4°C (as dictated in the manufacturer's provided protocol – *Rapid DNA Ligation Kit, Roche Diagnostics GmbH, Germany*).

Table V: Composition of alkaline phosphate treatment.

Reagents	Volume
CutSmart Buffer (10X)	2µl
Template	1-2µg
CIP	1unit per 1µg
wHPLC	Up to 20µl
Total volume	20µl

Table VI: The ligation reaction composition.

Reagents	Volume
Plasmid (Vector)	200ng
Insert	1000ng
Buffer (10X)	1 μ l
T4 ligase	1 μ l
wHPLC	Up to 10 μ l
Total volume	10μl

The next day, a fixe volume of ligation mixture was transformed into competent *E.coli* bacterial cells. Firstly, 45 μ l aliquots of competent cells (stored in -80°C) were placed on ice for 10 minutes. Thereafter, 5 μ l of the ligation product was mixed with the competent cells and further incubated on the ice for 15 minutes. To disrupt the bacterial membrane and to enable plasmid entry to the bacteria (*i.e.* transformation), the cells were subject to heat-shock on the preheated 42°C heat block for 90 seconds and subsequently placed back on ice for another 10 minutes. To aid bacterial recovery and allow sufficient time for successfully transformed bacteria to express the plasmid (pEasyFusion-mCherry – see appendix, Figure 33) encoded ampicillin resistance selection gene (*amp^r*), 250 μ l of pre-warmed SOC broth (Super Optimal broth with Catabolite repression) was added and placed again into a shaking heat block set at 37°C, for 30 minutes. Following brief centrifugation in a desk top microfuge, the resuspended bacterial pellet was spread over the surface of sterile LB agar plates (in a residual volume of SOC broth), containing the required antibiotic for selection of successful transformants (in this case with *Ampicillin* resistance; concentration= 100 μ g/ml), and incubated at 37°C, overnight (upside down to prevent any formed condensation forming on the LB agar surface). The numbers of resulting colonies on plates transformed with plasmid ligated in the presence of 5'/3' homology arm inserts or without insert, were compared to ensure the numbers were higher in the experimental condition versus basal control. A selection of experimental condition bacterial colonies were then streaked (in short straight streaks; ~20 numbered colonies per plate) out on new LB agar plates (containing the same antibiotic) and again incubated at 37°C for another 12-20 hours (until growth along the streak was observed). To identify which transformants contained the plasmid vector with the desired incorporated specific inserts (*i.e.* to confirm the successful ligation of a specific homology arm) colony-PCR was performed. Firstly, using a small sterile pipette tip, a small amount from each of bacterial streak was transferred to 50 μ l HPLC water and then heated to 96°C for 20 minutes

to liberate the plasmids from the clonal population of compromised bacterial cells. 1µl this lysate was then used as template for subsequent colony-PCR reactions using one of two specific primer combinations (either: i. T3 and T7 primers, recognising sequences that flank the insert sites used to confirm successful ligation of an insert by PCR product size. ii. a target gene-specific sense/antisense primer + T3/T7 primer on the plasmid backbone to confirm the correct orientation of the insert, as a viable PCR product would only be possible if the insert was cloned into the plasmid vector in the correct orientation). The colony-PCR reaction itself was performed using 2X DreamTaq™ Green PCR Master Mix (Thermo Scientific) in a total reaction volume of 5µl per 1 colony. The typical composition of the colony PCR reaction, primer sequences specific (10µM) for particular genes/plasmids and PCR programme are displayed in Tables VII, I/VIII, and IX, respectively). Note, that for each individual set of colony-PCRs performed, both positive (where possible – *i.e.* using pEasyFusion_mCherry with T7 and T3 PCR primers) and negative/positive controls (*i.e.* using pure HPLC water instead of bacterial lysate or plasmid as template, respectively) were included. Traced individual colony-PCR reactions were electrophoresised on 1% agarose gels and observed product size, against that theorised, were used to determine the success or otherwise of the cloning of the required insert (*i.e.* gene specific 3'/5' homology arm). Those colony-PCR products confirming successful cloning were then traced back to the original colony smears, that themselves were used as inoculum for 6ml LB broth medium (Invitrogen) cultures containing the appropriate antibiotic for selection growth and expansion of the plasmid containing clone (in this case, *Ampicillin* at a final concentration of 100µg/ml; a 1:1000 dilution of the -20°C stored stock). Such cultures were incubated in a shaking incubator (220 r.p.m.) at 37°C, overnight (still in the exponential growth phase). The next day a 500µl volume of expanded bacterial culture was mixed with an equal volume of 50% glycerol solution to create a long-term compatible clonal glycerol-stock, for storage at -80°C. The remainder of the bacterial culture was subject to plasmid isolation in readiness to confirm the correctness of the incorporation of the cloned insert via the conventional Sanger (dideoxynucleotide terminating) sequencing methods (commercial service - NextGEN). The plasmid extraction was conducted using a small-scale commercial plasmid isolation kit (QIAprep Spin Miniprep Kit; QIAGEN) according to the manufacturer's protocol. The concentration of purified/isolated plasmid was measured by UV spectrophotometry (Nanodrop) and sent for the out-sourced sequencing utilising several sequencing primers, as required (see Table IX) to confirm if the correct insert sequence was present (without deletions, insertions or single

nucleotide mutations) and in the correct orientation. The isolated plasmids with confirmed veracity were then either used as vectors to incorporate the missing gene specific 5'/3'homology arm or, in the case of a complete plasmid containing the mCherry cDNA sequence flanked by confirmed gene specific 5' and 3' homology arms, used as template in BIO-PCR reactions (see below) to generate the required biotinylated dsDNA HDR templates needed for single mouse embryo blastomere microinjection and *in situ* genome editing (see below).

Table VII: Colony-PCR composition for 1 colony.

Reagents	Volume
2X DreamTaq polymerase	2.5µl
Reverse primer	0.25µl
Forward primer	0.25µl
Template	1µl (50-100ng)
wHPLC	1µl
Total volume	5µl

Table VIII: PCR programme used for the verification insert cloning. *The elongation time depends on the size of PCR product (i.e. inserted 3'/5' homology arm).

PCR program	temperature	time
denaturation	95°C	2'
denaturation	95°C	30''
annealing	58°C	30''
elongation	72°C	2-4 *
extension	72°C	10'
cooling	4°C	∞

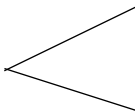
38x 

Table IX: Single sequencing primers T3 and T7 are complementary to the donor plasmid backbone sequence (used also to verify if the insert is cloned). mCherry-R/F are from the mCherry sequence to verify the correctness of the cloned product.

Primer	Sequence
T3	GCAATTAACCCTCACTAAAGG
T7	TAATACGACTCACTATAGGG
mCherry-R	TTGGTCACCTTCAGCTTGG
mCherry-F	CCCCGTAATGCAGAAGAAGA

After the successful cloning and the sequence verification of the 3'-homology arm for *Wwc2* (Frederica's work) and *Mapk13*, the 5'-homology arms were cloned using either a *EcoRV* (i.e. for *Wwc2*) or *EcoRI* (i.e. for *Mapk13*) based on the digestion strategy of the already confirmed vector. For *Mapk14* gene, the 5' arm (including *EcoRI* restriction enzyme) was cloned first, and subsequently (after sequencing verification) the 3'-homology arm (using the restriction enzyme *BamHI*) was cloned into the pEasyFusion_mCherry plasmid (using the same procedure as mentioned above).

3.1.3. Production of BIO-PCR dsDNA HDR template for CRISPR-Cas9 mediated genome editing (by homologous recombination)

To generate the required target gene specific dsDNA HDR templates, the previously constructed/modified pEasyFusion_mCherry plasmids (containing mCherry cDNA flanked by target gene specific 5'/3' homology arms corresponding to *Wwc2*, *Mapk13* and *Mapk14* genes – see above) were used as templates in BIO-PCR reactions resulting in 5'-biotinylated dsDNA HDR templates necessary for mouse embryo blastomere microinjection. Accordingly, the composite (5' homology arm- mCherry cDNA- 3' homology arm) inserts were PCR-amplified using universal primers complementary to the vector/plasmid backbone sequence, that also contained a custom 5'-biotin modification (Table X). Such BIO-PCR reactions were performed using High Fidelity Phusion DNA Polymerase (New England BioLabs) in a total reaction volume of 50µl. The composition of PCR reactions was the same as described in the section regarding the preparation of target gene specific homology arms (3.1.1.) and the PCR machine cycling conditions are described in Table XI. The correct size of the derived BIO-PCR products was confirmed by electrophoresis on 1% agarose gels. Subsequently, the BIO-PCR products were subject to QIAquick PCR purification kit (Qiagen) isolation, followed by ethanol precipitation, overnight (as described in section 3.1.2.). The obtained DNA pellets were resuspended in ~25µl volume of HPLC water, verified once again using agarose gel electrophoresis and the yield of derived biotinylated dsDNA HDR template, suitable for mouse embryo blastomere microinjection, was determined by Nanodrop.

Table X: Universal biotinylated PCR primers used in BIO-PCR to produce dsDNA HDR template that is biotinylated (at 5' ends, to facilitate successful *in situ* genome editing initiated by chromosomal DNA double-strand breaks catalysed by streptavidin-Cas9). Note, primer sequences are complementary to the pEasyFusion_mCherry plasmid backbone and result in the generation of biotinylated dsDNA HDR templates of a size equal to that of the 5'arm + 838bp (mCherry cDNA) + 3'arm.

Primer	Sequence
Bio-pcr sense primer	*AGGGAACAAAAGCTGGGTACCG
Bio-pcr antisense primer	*ATAGGGCGAATTGGAGCTCCAC

Table XI: PCR program used in BIO-PCR mediated generation of biotinylated dsDNA HDR templates.

PCR program	Temperature	Time
denaturation	98°C	2'
denaturation	98°C	30''
annealing	58°C	30''
elongation	72°C	4'
extension	72°C	10'
cooling	4°C	∞

38x

To obtain only one BIO-PCR product (with expected size), generated BIO-PCR products were digested with the restriction enzyme *DpnI* for 1 hour or overnight (Table XII). The digestion with the restriction enzyme *DpnI* results in the selective cleavage of methylated plasmid derived DNA, of bacterial origin, but does not target non-methylated PCR products.

Table XII: The reaction composition of the restriction enzyme digestion.

Reagent	Volume
Cut Smart Buffer (10X)	5µl
Template (BIO-PCR products)	2 µg
Restriction enzyme <i>DpnI</i>	1µl
HPLC water	up to 50µl
Total volume	50µl

3.2. Gene specific single guide sgRNA production

3.2.1. Cloning of target gene-specific oligos (complementary to sgRNA) into pX330-U6-Chimeric_BB-CBh-hSpCas9 plasmid

To produce target gene specific single-guide RNA (sgRNA) molecules for the microinjection into preimplantation mouse embryo blastomeres, a complementary pair of 24 nucleotide long DNA oligos (one per targeted gene: *Wwc2*, *Mapk13* and *Mapk14* - Sigma-Aldrich, with homology to genomic loci proximal to the targeted gene STOP codon) were cloned into the plasmid pX330-U6-Chimeric_BB-CBh-hSpCas9 (obtained from Addgene, clone number: 42230, see appendix for plasmid map, Figure 34). Afterwards, the recombinant plasmids were used to derive sgRNA by *in vitro* transcription (IVT). The sgRNA homologous and complementary oligos sequences were designed to create (after annealing, to derive a double-stranded oligo-hybrid; *i.e.* one per targeted gene) a 4 nucleotide 5'-overhang on each strand, that would be complementary to the overhangs created by the restriction enzyme digest of pX330-U6-Chimeric_BB-CBh-hSpCas9 using the *BbsI* restriction enzyme (therefore, permitting efficient cloning of the oligo-hybrid into the vector, that itself is unable to relegate as the generated *BbsI* overhangs on each strand are not complementary/compatible). The design of the annealed oligos also incorporated a central 20 nucleotide long double stranded section that is complementary to the target gene loci sequence (*i.e.* in our case around the targeted gene STOP codon). The oligo sequences used to generate the required inserts are displayed in Table XIII and were predesigned by my supervisor, doc. Bruce (incorporating the rules relating to Type-II Cas9 mediated genome editing, *i.e.* location of the PAM sequence relative to the 20 nucleotides of target gene loci homology, set out in the paper of Gu *et al.*, 2018). In order to anneal the two single stranded oligo components of the sgRNA complementary sequence, 50 μ l oligo containing solutions were prepared for each targeted gene (the composition of the reaction seen in Table XIV) and heated to 95°C in a PCR machine for 3 minutes, followed by natural/gradual cooling down to room temperature after 3 hours (*i.e.* switching the PCR block off). The concentration of created annealed oligos was then measured by UV spectrophotometry (Nanodrop).

Table XIII: The targeted gene specific sgRNA complementary oligo sequences, with homology to the intended site of Cas9 mediated genome editing (*i.e.* proximal to the STOP codon of the last exon – lower case), that were annealed and resulted in *BbsI* compatible overhangs (uppercase letters) for cloning into the plasmid pX330-U6-Chimeric_BB-CBh-hSpCas9.

Oligo name	Sequence
WWC2 sense	CACCgcagggtcacacgtcgtcag
WWC2 antisense	AAACctgacgacgtgtgacctgc
Mapk13 sense	CACCcatgaagctgcagtgattga
Mapk13 antisense	AAACtcaatcactgcagcttcag
Mapk14 sense	CACCgaaatggagtcctgagcacc
Mapk14 antisense	AAACggtgctcaggactccatttc

Table XIV: The composition of the annealing oligos reaction.

Reagents	Volume
sgRNAsense	1.5µl
sgRNA_antisense	1.5µl
HPLC water	47µl
Total volume	50µl

The purchased pX330-U6-Chimeric_BB-CBh-hSpCas9 plasmid (that came as a live bacterial agar stab) was used as inoculum in a 6mL LB (+*Ampicillin*). It was cultured overnight (37°C + 220 r.p.m. shaking) and subsequently extracted/purified, using a commercial plasmid isolation kit (QIAprep Spin Miniprep Kit; QIAGEN), according manufacture’s protocol (concentration measured by UV spectrophotometry - Nanodrop). Thereafter, the plasmid was linearized via two adjacent restriction sites for *BbsI* (thus avoiding the possibility of plasmid self-ligation) at 37°C, overnight. The *BbsI*+ pX330-U6-Chimeric_BB-CBh-hSpCas9 reaction mixture is given in Table XV. Digested plasmid was electrophoresed on a 1% agarose gel (+ethidium stain) to confirm the correct linearized size and quantified by UV spectrophotometry (Nanodrop). Uncut plasmid was also resolved on the same gel to provide a means of comparison to further confirm successful linearization. Subsequently, the linearized plasmid was purified using a conventional phenol-chloroform extraction protocol, as described above (the section 3.1.2.), followed by ethanol precipitation. The concentration of the purified plasmid was confirmed by UV spectrophotometry (Nanodrop).

Table XV: The reaction composition of the restriction enzyme digestion for pX330-U6-Chimeric_BB-CBh-hSpCas9 (used as a template).

Reagent	Volume
NEBuffer™ 2:1	5µl
Template (plasmid)	2 µg
Restriction enzyme <i>BbsI</i>	1µl
HPLC water	up to 50µl
Total volume	50µl

The linearized pX330-U6-Chimeric_BB-CBh-hSpCas9 plasmid and the generated target gene specific annealed and hybrid sgRNA complementary oligonucleotides were ligated together using a T4 DNA ligase enzyme (Roche Diagnostics – as directed in the manufacturer’s protocol and adhering to published standard molar ratios, the available online NEBio calculator tool (<https://nebiocalculator.neb.com/#!/ligation>)). Subsequently, it was followed by transformation into competent *E.coli* cells. The processes of ligation and transformation were performed exactly as describe above in the section 3.1.2 and Table VI. The resuspension of transformed cells was spread over LB agar plates (containing *Ampicillin* for selection of successful transformants with the concentration used 100µg/ml) and incubated at 37°C overnight. Resulting bacterial colonies were processed for colony-PCR as described above in the section 3.1.2., and in Tables VII, VIII (expect for elongation time which was 1 minute based on the PCR product size). The colony-PCR products used PCR primers complementary to plasmid backbone (Table XVI). Thus, those clones harbouring a pX330-U6-Chimeric_BB-CBh-hSpCas9 plasmid with the desired target gene sgRNA complementary/specific insert were identifying. Note that the design of the cloning procedure ensured the inserts could only be cloned in the correct orientation – in contrast to the cloning of target gene specific 5’/3’ homology arms into pEasyFusion_mCherry, as described above. The correct anticipated sizes of PCR products were examined by the gel electrophoresis using a 2% agarose gel.

Table XVI: The primers (complementary to plasmid backbone) used in a PCR reaction to confirm the presence of cloned insert.

Primer	Sequence
Sense	GCATATACGATACAAGGCTGTTAGA
Antisense	CCGTAAGTTATGTAACGGGTACCTC

Once confirmed, by visualization of a PCR product with expected size on an electrophoresed agarose gel, plasmids were isolated (from 6ml LB cultures inoculated with bacteria from the originally streaked colony PCR replica plate) and purified using a commercial plasmid isolation kit (QIAprep Spin Miniprep Kit; QIAGEN), according to the manufacturer's instructions (plasmid concentration determined using UV spectrophotometry - Nanodrop). All derived pX330-U6-Chimeric_BB-CBh-hSpCas9 plasmids containing target gene sgRNA specific/complementary inserts were sequence verified by out-sourced dideoxynucleotide sequencing (NextGEN) using several sequencing primers, as required (see Table XVI).

3.2.2. Generation of sgRNAs by IVT

Next the target gene specific sgRNA coding sequences were PCR-amplified from the pX330-U6-Chimeric_BB-CBh-hSpCas9 plasmids using the following primers; i. the sense/forward primer incorporating a 5'-T7-RNA polymerase promotor sequence, immediately followed by a region complementary to the start of the cloned oligo-derived sgRNA complementary sequence (and was therefore unique for each of the three targeted genes; *Wwc2*, *Mapk13* and *Mapk14*), and, ii. an anti-sense/reverse primer that was complementary to the pX330-U6-Chimeric_BB-CBh-hSpCas9 vector and was hence universal. The adoption of these PCR primers ensured any product would contain a 5'-T7-RNA polymerase promotor sequence that could be utilised in IVT to derive the target gene specific sgRNA (comprising the 20 nucleotides of target gene loci complementarity, to ultimately target the Cas9 complex to the correct genomic region, and the necessary tracrRNA like sequence that facilitates the incorporation of the sgRNA into the Cas9 protein). All PCR primers used to generate the required dsDNA IVT template (incorporating the T7 promotor sequence) are shown in Table XVII. The PCR conditions are displayed in Table XVIII and the PCR composition was used as it is described in the section 3.1.1.

Table XVII: PCR primers used to generate dsDNA encoding sgRNA templates for IVT using T7 RNA polymerase (note, the T7-RNA-polymerase promoter sequence in target gene specific forward primers are highlighted in bold text, the lowercase letters correspond to part of the target gen loci specific/complementary region).

Primer	Sequence
T7_Mapk14 sense	TAATACGACTCACTATAGG gaaatggagtcctgagcacc
T7_Mapk13 sense	TAATACGACTCACTATAGGG catgaagctgcagtgattga
T7_Wwc2 sense	TAATACGACTCACTATAGG gcagggtcacacgtcgtcag
Universal reverse primer to generate sgRNAs	AAAAGCACCGACTCGGTGCC

Table XVIII: PCR conditions for the generation of required dsDNA as IVT template (incorporating the T7 promoter sequence).

PCR program	Temperature	Time
denaturation	98°C	2'
denaturation	98°C	30''
annealing	58°C	30''
elongation	72°C	30''
extension	72°C	10'
cooling	4°C	∞

38x

The derived target gene specific T7-RNA-polymerase promoter containing sgRNA encoding PCR products were gel extracted according to the isolation kit protocol (GenElute™ Gel Extraction Kit, Sigma). Gel extracted PCR products were then ethanol precipitated (as described in the section 3.1.2.) and resuspended in a ~25µl volume of HPLC-grade water. Their concentration was determined by UV spectrophotometry – Nanodrop. 0.1-0.2µg of each target gene specific purified sgRNA encoding dsDNA PCR product were then used as template in IVT reactions, utilising a T7 transcription kit (MEGAscript™ T7 transcription kit, ThermoFisher Scientific) to generate the desired sgRNA constructs. IVT reactions were performed as instructed in manufacture’s protocol and included an incubation time of 4 hours at 37°C. The IVT reaction mixture was prepared as is shown in TableXIX. Post-synthesis, the derived sgRNA preparations were pulse spun in a bench top microfuge and 1µl of Turbo DNaseI (from the MEGAscript™ T7 transcription kit) was added and left for further 20 minutes incubation at 37°C (to remove the PCR generated IVT template). The integrity of derived *Wwc2*-, *Mapk13*- and *Mapk14*-specific sgRNA constructs were confirmed by

conventional non-denaturing agarose gel electrophoresis. The derived sgRNA constructs were purified by phenol-chloroform extraction for RNA inserts, but utilising pH 5.2 Tris saturated phenol:chloroform (the procedure was the same as described above in section 3.1.2). Afterwards, they were precipitated with 600µl isopropanol and 30µl of 3M NaAc (pH 5.2), overnight. After the precipitation, the samples were centrifuged for 35 minutes (in a pre-cooled centrifuge, 4°C). The pellets were washed 3 times, with 70% ethanol (500µl). The dried pellets were resuspended with a ~25µl volume of Nuclease-free water. The concentration of derived sgRNAs were then quantified by UV spectrophotometry (Nanodrop) and individual constructs were stored at -80°C until required for later embryo blastomere microinjection.

Table XIX: The IVT reaction mixture for a T7 transcription kit.

Component	Volume
Nuclease-free Water	to 20 µL
ATP solution	2 µL
CTP solution	2 µL
GTP solution	2 µL
UTP solution	2 µL
10X Reaction Buffer	2 µL
PCR-product template	0.1–0.2 µg
Enzyme Mix	2 µL

3.3. Generation of Cas9-streptavidin mRNA

The Cas9-Streptavidin single stranded mRNA was generated as the third component to be microinjected into mouse embryo blastomeres and required to mediate CRISPR-Cas9 mediated *in situ* genome editing. Hence, it was necessary to purchase the plasmid, pCS2⁺-Cas9-mSA (obtained from Addgene, clone number: 103882, see appendix for plasmid map, Figure 35) containing the coding sequence of the Cas9 endonuclease gene (isolated from *Streptococcus pyrogenes*) and fused with a mSA sequence (monomeric streptavidin). It is necessary for biotin-streptavidin interaction and to facilitated genome editing using biotinylated dsDNA HDR templates as it was employed in this study and previously (Gu *et al.*, 2018)) to the C-terminus-encoding region of the *Cas9* coding sequence. Thus, after creating a -80°C storage glycerol stock of the purchased pCS2⁺-Cas9-mSA plasmid, it was amplified in a 6ml overnight LB shaking culture (37°C, 220 r.p.m., with 100µg/ml ampicillin, extracted and purified using a commercial plasmid isolation kit (QIAprep Spin Miniprep Kit;

QIAGEN), according to the manufacturer protocol. After quantification of the plasmid yield (Nanodrop UV spectrophotometer), 2µg of the isolated circular plasmid was linearized by a *NotI* restriction enzyme digestion (note, the unique *NotI* site is downstream of the Cas9-mSA coding sequence), by overnight incubation at 37°C (digestion components are described in Table XX). Successful pCS2⁺-Cas9-mSA linearization and verification of the correct size of the cut plasmid was confirmed by agarose gel electrophoresis, comparing cut and uncut plasmid preparations. The linearized plasmid was then purified by routine phenol-chloroform extraction followed by ethanol precipitation (as described above, section 3.1.1.). The final DNA pellet was resuspended in ~25µl volume of nuclease free water (based on the pellet size) and the concentration was measured by UV spectrophotometry (Nanodrop).

Table XX: Components and their appropriate volumes for *NotI* restriction enzyme digestion of pCS2⁺-Cas9-mSA plasmid: (µg) mikrogram, (µl) microlitre.

Reagent	Volume
CutSmart Buffer (10X) NEB	2µl
Purified uncut plasmid	1-2 µg
Restriction enzyme <i>NotI</i>	1µl
HPLC water	up to 20µl
Total volume	20µl

To obtain Cas9-mSA mRNA required for the mouse embryo blastomere microinjection, 1µg of the *NotI* linearized pCS2⁺-Cas9-mSA plasmid was used as template for an IVT reaction. Due to the presence of a plasmid vector encoded SP6 RNA polymerase promotor upstream of the Cas9-mSA coding sequence, the mMMESSAGE mMachine SP6 Transcription Kit (Thermo Fisher Scientific) was used. The IVT reaction was performed as instructed in the provided kit protocol, with an incubation time of 1 hour at 37°C. The IVT reaction mixture was prepared as shown in TableXXI, part A. Following the 1hour mRNA synthesis period, 1µl of Turbo *DNAseI* was added to the reaction mixture and incubated for further 20 minutes at 37°C (to remove the plasmid template). To verify the success of the IVT reaction, a 1µl aliquot of the reaction was processed by agarose gel electrophoresis (110V, 30 minutes) and the size of the mRNA IVT product determined. The remainder of the synthesized mRNA was subject to post-synthesis 3' poly-adenylation (Poly(A) Tailing Kit- ThermoFisher Scientific) according to the kit manufacturer's protocols (reaction components summarised in

Table XXI, part B) for 1 hour at 37°C. The poly-adenylated IVT product was then purified by routine phenol-chloroform extraction, followed by ethanol precipitation (as mentioned above) and resuspended in ~25µl volume of nuclease-free water. The integrity of the derived poly-adenylated Cas9-mSA mRNA was confirmed by denaturing agarose gel electrophoresis using glyoxal as the agent responsible for denaturation. Thereafter, the yield of Cas9-mSA mRNA IVT was quantified by UV spectrophotometry (Nanodrop). The mRNA was stored at -80°C until required for embryo blastomere microinjection.

Table XXI: Components and their appropriate volumes for *in vitro* transcription (IVT) (A) and poly-adenylation (Poly-A+ tailing) (B) of Cas9-mSA mRNA from *NotI* linearized pCS2⁺-Cas9-mSA plasmid: (µg) mikrogram, (µl) microlitre

A)

Reagent	Volume
Nuclease-free Water	up to 20µl
2X NTP/CAP	10µl
10X reaction buffer	2µl
Linearized plasmid	1µg
Total volume	20µl

B)

Reagent	Volume
IVT derived mRNA	20µl
Nuclease-free Water	36µl
5X E-PAP Buffer	20µl
25mM MnCl ₂	10µl
10mM ATP	10µl
E-PAP enzyme	4µl
Total volume	100µl

3.4. Preimplantation mouse embryo specific methods

3.4.1. Preimplantation mouse embryo cultivation

To obtain preimplantation mouse embryos for the experimentation (for the microinjection of the derived CRISPR-Cas9 reagents required for *in situ* genome editing at specific gene loci in mouse embryo blastomeres *i.e.* target gene specific biotinylated dsDNA HDR template and sgRNA constructs and Cas9-mSA mRNA), 8-9 week old F1 hybrid female mice (obtained from a C57BL6♀×♂CBA/W cross) were super-ovulated by intra-peritoneal injection of 7.5IU of PMSG (pregnant mare serum gonadotrophin extract; Sigma Aldrich-Merck). After 48 hours, the same F1 female mice were injected with 7.5IU of hCG (recombinant human chorionic gonadotrophic hormone; Sigma Aldrich- Merck) and

immediately placed with F1 males for the overnight mating (successful mating confirmed the next day by observing vaginal sperm plugs). 42 hours after hCG injection, the oviducts from super-ovulated and mated F1 females were dissected, and 2-cell stage embryos were isolated and recovered in M2 medium (pre-warmed at 37°C for at least 2-3 hours). The detailed composition of M2 media is shown in Table XXII. Obtained embryos were washed through several M2 drops (in a 35mm culture dish), covered with light mineral oil (Irvine Scientific), and used for future microinjection.

Table XXII: The concentration of stock M2 media components and their composition in the final prepared M2 media: (g) grams, (ml) millilitres, (mg) milligrams.

STOCK	M2 MEDIA ingredients	g/100ml	TOTAL VOLUME
A (x10)	NaCl	5.534	10.0ml
	KCl	0.356	
	KH ₂ PO ₄	0.162	
	MgSO ₄ ·7H ₂ O	0.293	
	Na-Lactate 60% syrup	3.2(ml)	
	Glucose	1.000	
	Penicilin	0.060	
	Streptomycin	0.050	
B (x10)	NaHCO ₃	2.101	1.6ml
	Phenol Red	0.010	
C (x100)	Na Pyruvate	3.600	1.0ml
D(x100)	CaCl ₂ ·2H ₂ O	2.520	1.0ml
E (x10)	HEPES	5.958	8.4ml
F	BSA		400(mg)
G	H ₂ O		78.0ml

After the co-microinjection of the specific targeted gene CRISPR-Cas9 reagents into 2-cell stage embryo blastomeres, the embryos were immediately transferred into commercially procured KSOM growth media drops (EmbryoMax® KSOM Mouse Embryo Media - Merck - either with or without additional amino acid (AA) supplementation, overlaid with light mineral oil in 35mm culture plate), washed through a series of further KSOM drops (to remove trace amounts of M2 media) and placed in an incubator set at 37°C with a 5% CO₂ atmosphere (note, KSOM media plates was prepared in advance and equilibrated in the incubator for at least 3-4 hours, prior to embryo transfer).

3.4.2. Cytoplasmic microinjection of preimplantation 2-cell-stage mouse embryos

All equipment necessary for the microinjection was prepared in advanced. Microinjection needles were prepared from filamented borosilicate capillary tubes (Harvard Apparatus – 30-008) using a Micropipette Maker machine (model PC-10 - Narishige). Holder pipettes were prepared manually (by flaming the end of non-filamented borosilicate capillary tubes - Harvard Apparatus 30-0017). The actual microinjection procedure was performed by a Ph.D. student, Rebecca Collier, and optimisation continues by Giorgio Virnicchi. The microinjection apparatus comprises four components: i.) a fluorescence inverted microscope (OLYMPUS IX71) used for the object observation ii.) FemtoJet (positive pressure) microinjection machine (Eppendorf) used to expel microinjection needle contents into the embryonic blastomere (*i.e.* the target gene specific CRISPR-Cas9 reagents; either under a constant pressure or a bolus of elevated injection pressure) iii.) Electrophysiology rig, used to run a current under negative capacitance from the microinjection needle, through the injection medium to the holding pipette (World Precision Instruments - WPI); required to assist the passage of the microinjection needle through the embryonic blastomere plasma membrane iv.) Oscilloscope (RS Components Ltd.), used to visualise the generated current. The three prepared CRISPR-Cas9 constructs/reagents, specific for either the *Wwc2* or *Mapk13* gene, were co-microinjected into one blastomere of freshly recovered 2-cell stage embryos, on a concaved microscope slide containing M2 media overlaid with light mineral oil on the stage of the inverted microscope. Microinjection for of CRISPR-Cas9 reagents for both genes was performed several times with varying conditions and concentrations of Cas9-mSA mRNA, target gene specific sgRNA, and biotinylated dsDNA HDR templates, as described in Table XXIII, section 4.4. Some microinjections were performed with the addition of an injection marker mRNA encoding the recombinant fluorescent fusion plasma-membrane marker protein GAP43-GFP (60ng/ μ l) to the microinjection mixture (thus allowing a judgement of the success of the microinjection procedure by the presence of plasma membrane localised GFP fluorescence; ~2 hours post-microinjection) or EGFP (60ng/ μ l) present in cytoplasm of embryo. Microinjected embryos were transferred into pre-equilibrated KSOM growth media drops/plates and *in vitro* cultured until an appropriate cell stage to assay for successful genome editing in the microinjected blastomere based on the expression of targeted genes fused to mCherry (from the edited endogenous locus).

3.4.3. Embryo fixation and DAPI counter-staining

Prior to fixation, microinjected preimplantation stage embryos at the desired developmental stage were washed through several drops of pre-warmed (37°C) M2 media, before being transferred to a drop of acid Tyrode's solution (Sigma) to remove the *zona pellucida* (as judged by continual visual inspection using a dissecting stereo-microscope). Then, they were washed again through several pre-warmed M2 drops. Embryos were then immediately transferred to a well of a 96-well micro-titre plate containing a 4% paraformaldehyde solution (PFA, Santa Cruz Biotechnology) and fixation was permitted for 20 minutes at 37°C. Thereafter, the embryos were washed through 3 wells of 0.15% PBST (Phosphate buffered saline with 0.15% Tween 20) and remained in the last well for 20 minutes at room temperature. Afterwards, embryos were transferred into DAPI containing Vectashield mounting medium (Vector to fluorescently counterstain blastomere nuclei/DNA). Prepared fixed embryos were then either immediately visualised under fluorescence confocal microscopy or stored at 4°C prior to later microscopic visualisation.

3.4.4. Confocal microscopy and image analysis

Microinjected, fixed and DAPI counter-stained embryos (prepared as described above) were placed in small Vectorshield drops on the surface of glass coverslip bottomed 35mm culture plates (Matek) and overlaid with mineral oil. The prepared plates were then placed (using the appropriate mount) on the stage of an inverted confocal microscope (Olympus FLUOVIEW FV10i). After focussing on the fixed and mounted embryos (using the bright field differential interference channel), laser excitation and detector emission wave lengths (utilising standard filter settings) were set to record mCherry and DAPI derived fluorescence (or in the case of embryos also microinjected with recombinant microinjection marker *Gap43-GFP/EGFP* mRNA, additional GFP fluorescence). All embryos were scanned as a complete z-series of high-resolution images (in each appropriate channel), with a small z-intervals (2µm). The individual power settings of the of the laser and sensitivity of detectors were adjusted according to each experiment (in order to maximise mCherry derived target gene fusion protein expression detection). The images of microinjected embryo blastomeres were captured within the Olympus FluoView V4.1a Viewer (Olympus) software analysis and edited automatically using Imaris X64.

4. Results

Before my arrival to the laboratory, a previous ERASMUS student, Frederica Serati, had already successfully cloned 3' homology arm of the *Wwc2* gene locus into the pEasyFusion_mCherry vector and the target gene specific component of the sgRNA of the same gene into pX330-U6-Chimeric_BB-CBh-hSpCas9 plasmid. Therefore, I continued her work from this point, as described below (hence, the results such as gel pictures *etc.*, relating to the cloning of the 3' homology arm of the *Wwc2* gene into pEasyFusion_mCherry and the corresponding cloning of the target gene specific component of the *Wwc2* gene sgRNA are not described in this thesis).

4.1. Preparation of biotinylated recombinant DNA repair templates for *Wwc2*, *Mapk13* and *Mapk14* genes

To enable the homology-directed repair (HDR) pathway component of the CRISPR-Cas9 genome editing procedure, biotinylated recombinant DNA repair templates, (each specific for a certain gene *i.e.* *Wwc2*, *Mapk13* and *Mapk14*) were derived. Each dsDNA HDR template consisted of a mCherry coding sequence (the fluorescence tag) flanked by gene specific homology arm sequences (*i.e.* a 5' arm and a 3' arm), incorporating 5'-biotin modifications on each strand. This would, after successful gene editing, results in the endogenous target gene loci being modified by the removal of the original STOP codon and being replaced by an in-frame fusion of the last exon with the mCherry fluorescent reporter (complete with its own STOP codon). Thus, it leads to the generation of the required reporter, expressed from the endogenous gene loci.

To generate biotinylated dsDNA HDR template, it was necessary to clone the two gene specific homology arm inserts, each with 100% sequence identity to ~1.2Kb fragments immediately around the appropriate target gene STOP codon, either side of the mCherry coding sequence in the plasmid pEasyfusion-mCherry. Thereafter, a BIO-PCR reaction (using 5'-biotin modified forward and reverse oligos) could be performed to produce a biotinylated dsDNA HDR template for mouse embryo blastomere microinjection (note, dsDNA HDR template was biotinylated to achieve a higher efficiency of genome editing, given the Cas9 to be used is fused to monomeric streptavidin, promoting one of the strongest non-covalent interactions, between Cas9 and dsDNA HDR template, known - see Figure 7.).

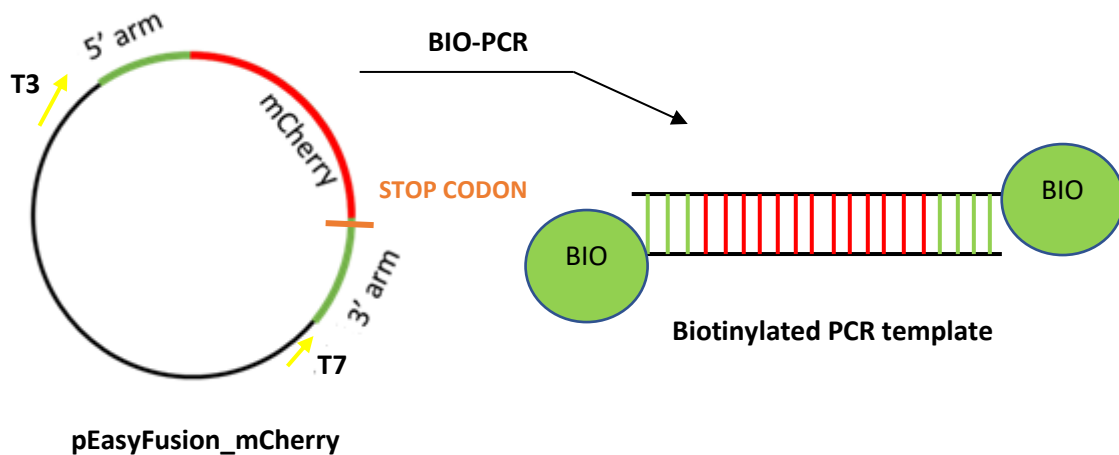


Figure 7. A scheme of the generation of target gene specific biotinylated dsDNA HDR template for use in genome editing to create C-terminal mCherry reporter fusion genes. The sequences of both target gene 5' and 3' homology arms (immediately flanking the original STOP codon and ~1.2 Kb in length) were cloned, in-frame, upstream (5' arm) and downstream (3' arm) of the mCherry cDNA sequence of the plasmid, pEasyFusion_mCherry. After sequence verification, the dsDNA HDR template was amplified by BIO-PCR in preparation for mouse embryo blastomere microinjection.

4.1.1. Cloning of gene specific 3' and 5' homology arms (i.e. *Wwc2*, *Mapk13* and *Mapk14*) into pEasyFusion_mCherry vector

For the cloning of the 5' arm of *Wwc2* gene, three different designed PCR primers pairs were used (incorporated 6 nucleotide spacer sequences at their 5' end followed by either *EcoRI*, *HindIII* and *EcoRV* restriction enzyme recognition sequences sites to facilitate cloning into the correct mCherry cDNA flanking region of the pEasyFusion_mCherry vector). However, only those PCR primers pairs which contained the *EcoRV* sites were useful. The derived PCR products using primer pairs incorporating *EcoRI* or *HindIII* indicated the presence of these sites in PCR product itself (not previously identified in the available genomic DNA sequence). For brevity, I have only presented the gel images for the *EcoRV* linked variant of the *Wwc2* gene specific 5' homology arm PCR product (Figure 8, part C), together with those derived for the 5'/3' homology arms for the *Mapk13* and *Mapk14* genes (each amplified with primers incorporating *EcoRI* and *BamHI* restriction enzyme recognition sequences, for cloning of the 5' and 3' homology arms, respectively – Figure 8 A & B).

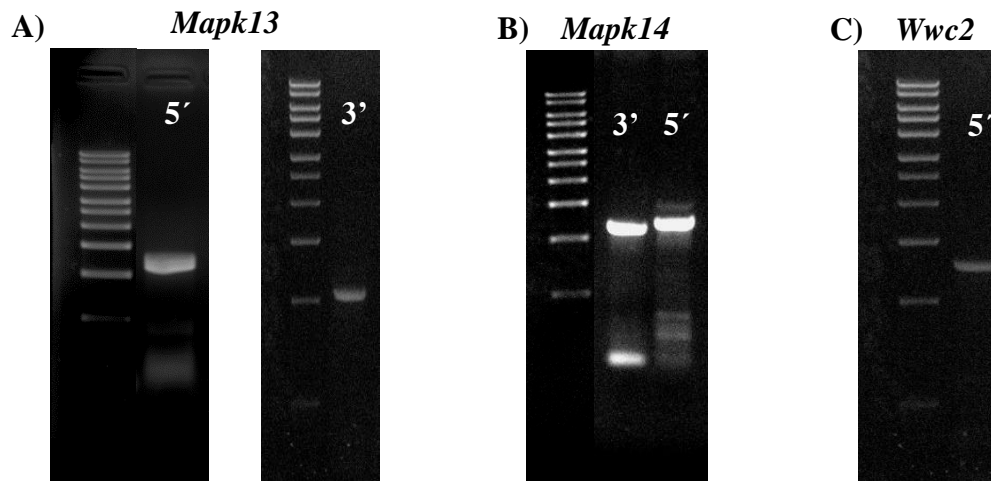


Figure 8. Amplified mouse genomic DNA PCR products to be cloned as 5' and 3' gene-specific homology arms into pEasyFusion_mCherry vector. A) *Mapk13* gene 5' homology arm (left), primers annealing temperature: 68°C and expected product size: 1158bp, and 3' homology arm (right), primers annealing temperature: 62°C and expected product size: 1073bp. **B)** *Mapk14* gene and its 3' homology arm (second lane), primers annealing temperature: 62°C and expected product size: 1137bp, and 5' homology arm (first lane), primers annealing temperature: 62°C and expected product size: 1258bp. **C)** *Wwc2* gene with its 5' homology arm, primers annealing temperature: 63°C and expected product size: 1262bp. In all three cases, the gel electrophoresed marker lane contains a 1Kb ladder marker for size reference (from top to bottom: 10, 8, 6, 5, 4, 3, 2.5, 2, 1.5, 1 & 0.5 Kb).

However, as is visible on the gels, some unspecific products were present along with the correct PCR product (*i.e.* primer-dimers or/and spurious PCR products with smaller sizes). Therefore, as an extra precaution (regarding the subsequent insert cloning steps) the correctly sized/anticipated bands were directly extracted from minimal gel slices, at the following final concentrations: *Mapk13* (5': 60.9ng/μl, 3': 59ng/μl), *Mapk14* (5': 53.5ng/μl, 3': 55.1ng/μl) and *Wwc2* (5': 48.6ng/μl). These gel extracted PCR products were then used as template in specific restriction enzyme digestions (to create the sticky/cohesive ends required for cloning into the pEasyFusion_mCherry vector) using the appropriate/relevant restriction enzyme for the generated insert (as described above, Table I). The digested PCR products were purified using a PCR purification kit to yield insert digests with the following concentrations: *Mapk13* (5': 25.3ng/μl, 3': 51.4ng/μl), *Mapk14* (5': 56.5ng/μl, 3': 39.3ng/μl) and *Wwc2* (5': 39.6ng/μl).

In readiness to clone the prepared inserts, the pEasyFusion_mCherry plasmid vector was linearized with insert appropriate restriction enzymes (*i.e.* the same one as the intended insert had been pre-digested with) and then alkaline phosphatase treated (to prevent subsequent self-ligation). Thus, the isolated and purified pEasyFusion_mCherry plasmid (3663bp – or the version already containing the 3' homology arm of the *Wwc2* gene) were digested/linearized, utilising appropriate restriction enzyme recognition sequences that were on one or the other flanking side of the mCherry cDNA component. Successful linearization was confirmed by agarose gel electrophoresis (Figure 9).

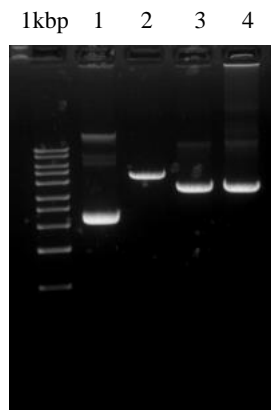


Figure 9. Verification of the successfully linearized pEasyFusion_mCherry plasmids after specific restriction enzyme digestion. The pEasyFusion_mCherry plasmid was digested with relevant restriction enzymes relating to the same restriction enzyme used for gene specific genomic DNA inserts (as shown in Table I). **1)** Undigested pEasyFusion plasmid (note, the three bands detail the presence of nicked, supercoiled and circular forms of the plasmid). **2)** Plasmid incorporating the 3' homology arm of *Wwc2* gene (4724bp) after digestion with *EcoRV*. **3 & 4)** Linearized plasmid (3663bp), digested with *EcoRI* and *BamHI* restriction enzymes, respectively. All plasmids correspond to the correct expected sizes. A 1Kb ladder marker is shown for size reference (from top to bottom: 10, 8, 6, 5, 4.3, 2.5, 2, 1.5, 1 & 0.5 Kb).

Directly after linearization, all pEasyFusion_mCherry plasmids were alkaline phosphatase treated and then purified by phenol-chloroform extraction and ethanol precipitation to the following concentrations: i. *EcoRV* digested pEasyPhusion_mCherry already containing the 3' arm of the *Wwc2* gene, 301.6ng/μl, ii. & iii. pEasyPhusion_mCherry vectors digested with *EcoRI* and *BamHI*, 314ng/μl and 419.9ng/μl, respectively. The linearized plasmids were then ligated with the appropriately digested genomic DNA derived PCR product inserts and transformed into competent *E-coli* bacteria and plated on LB agar under antibiotic selection (*Ampicillin*). The resulting colonies were then screened for successful insert ligation into pEasyFusion_mCherry plasmid by colony PCR (when in

numbers exceeding the basal number of colonies derived from ligation without insert). According to the strategy, all colonies were first screened using universal T3 and T7 primers (annealing to sites in the plasmid backbone, flanking the intended insert site). If a PCR product of the correct size was generated and visible on an electrophoresed agarose gel, the same colony would be subject to a second round of colony PCR using primers pairs that corresponded to the insert itself and one of the universal priming sites. If this yielded a PCR product of the anticipated size, this would indicate the insert was cloned in the correct orientation (as it would not be possible to derive a product if it were inserted with the opposing orientation). Such colonies were retained and the plasmids extracted from them sent for sequence verification of the correct cloning of the insert. More details can be found in Materials and Methods (the section 3.1.2.).

I shall now in turn summarise the colony PCR based screening of the cloning of 5' and 3' homology arms, into pEasyFusion_mCherry, for each of the three targeted genes (*i.e.* *Wwc2*, *Mapk13* and *Mapk14*).

4.1.1.1. *Wwc2* gene 5' homology arm cloning

In the case of the *Wwc2* gene, it was only necessary to clone the 5' homology arm. Figure 10, gel A shows the results of the initial colony PCR screen using the universal T3 and T7 PCR primers to confirm presence of the 5' homology arm insert with an expected size of 3178bp (*i.e.* comprising the mCherry cDNA sequence (708bp), the originally cloned 3' homology arm (1061bp) and newly inserted 5' homology arm (1262bp)). These positive colonies were then screened in a second colony PCR using the vector encoded T3 primer and antisense primer originally used to derive the cloned insert itself (Figure 10, gel B). A PCR product band size of 1340bp verified the orientation of the cloned insert.

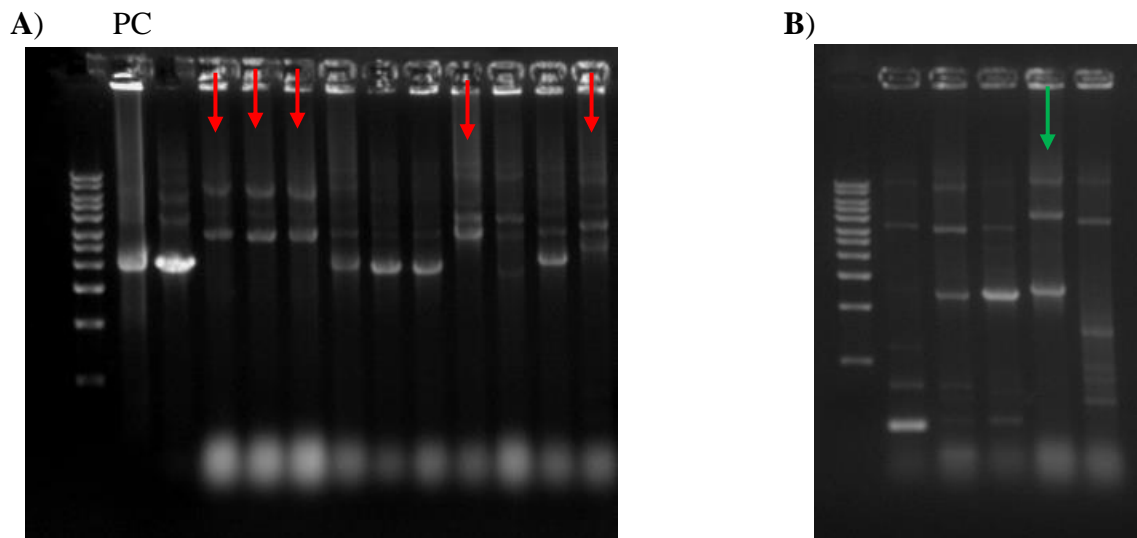


Figure 10. Agarose gels depicting 2-step colony PCR screening of pEasyFusion_mCherry containing clones (already containing the *Wwc2* gene 3' homology insert) with the successful insertion of the 5' homology arm (highlighted with a red/green arrow). **A)** Colony PCR conducted with universal T3 and T7 primers that yield a 3183bp product if the insert is present (highlighted by red arrows). Note a PCR positive control (PC) condition using the same T3 and T7 primers to amplify the original undigested pEasyFusion_mCherry plasmid with cloned 3' arm was included (expected band size 1916bp). **B)** Colony PCR performed with T3 and *Wwc2* gene 5' arm antisense primer to indicate of a correct orientation of the cloned insert. The expected size was 1340bp (*i.e.* from the T3 primer sequence till the antisense primer of 5' homology arm insert – highlighted by a green arrow and indicating individual clone sent for sequencing). 1Kb ladders marker are shown for size reference (from top to bottom:10, 8, 6, 5, 4,3, 2.5, 2, 1.5, 1 & 0.5 Kb).

Thus, the confirmed colony (marked with green arrow; Figure10, gel B), it was used to inoculate a small LB culture from which the pEasyFusion_mCherry vector containing both 5' and 3' homology arms from the *Wwc2* gene (flanking the central mCherry cDNA sequence) and purified with the final concentration 511.5ng/ μ l. Subsequently, it was sent for complete sequence verification of the insert (plus a glycerol stock for long-term storage in the lab's -80°C plasmid archive was prepared). Thus, the confirmed required template for later BIO-PCR, to synthesise the required biotinylated dsDNA HDR template for the planned *in situ* genome editing of the *Wwc2* gene was prepared for the microinjection into preimplantation mouse embryo blastomeres.

4.1.1.2. *Mapk13* gene 5' and 3' homology arm cloning

The linearized pEasyFusion_mCherry plasmid with *Bam*HI restriction enzyme was first ligated with the *Bam*HI digested 3' arm and the resulting colonies were similarly screened by colony PCR. Firstly, using universal T3 and T7 primers (Figure 11, gel A), with an expected/correct product size of 1928bp (*i.e.* including the mCherry and clone 3' homology arm). After detecting colonies with confirmed inserts, these were then screened in a second round of colony PCR to verify the appropriate orientation of insert (Figure 11, gel B). In this case, the utilised PCR primers were the vector complementary T7 universal primer and sense primer complementary to the *Mapk13* genomic loci used to generate the 3' homology arm. The anticipated product size was 1142bp. A confirmed clone was then expanded (stored as a -80°C glycerol stock) and the correctly modified plasmid isolated (732.2ng/μl) following by sequence verification.

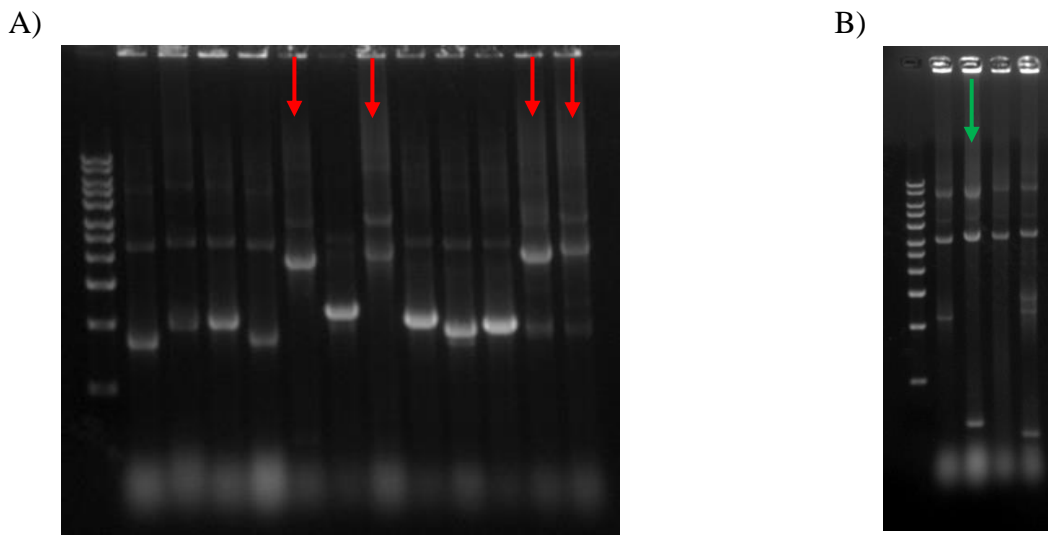


Figure 11. Agarose gels depicting 2-step colony PCR screening of pEasyFusion_mCherry containing clones for the successful insertion of the 3' homology arm of the *Mapk13* gene (highlighted with a red/green arrow). **A)** Colony PCR conducted with universal T3 and T7 primers that yield a 1928bp product if the insert is present (highlighted by red arrows). **B)** Colony PCR performed with T7 and *Mapk13* gene 3' homology arm sense primer to indicate of a correct orientation of the cloned insert. The expected size was 1142bp (*i.e.* from the sense primer of 3' homology arm insert till the T7 primer sequence – highlighted by a green arrow and indicating individual clone sent for sequencing). 1Kb ladders marker are shown for size reference (from top to bottom: 10, 8, 6, 5, 4, 3, 2.5, 2, 1.5, 1 & 0.5 Kb).

The resulting pEasyFusion_mCherry plasmid, containing the *Mapk13* gene 3' homology arm, was then linearized with *EcoRI*, in preparation of cloning the 5' homology arm (thus, completing the flanking of the mCherry cDNA sequence). The successful vector linearization of the purified plasmid (concentration 109.8ng/μl) was confirmed by agarose gel electrophoresis (Figure 12). The linearized vector was ligated with the pre-restriction enzyme digested (*EcoRI*) 5' homology arm PCR product insert, transformed, and plated. The resulting colonies were then screened by colony PCR. Firstly, using the universal T3 and T7 primers (expected/correct PCR product size was 3086bp, *i.e.* mCherry cDNA, plus both 5' and 3' homology arms of the *Mapk13* locus – *gel data not shown*) and then the positive colonies were screened using the universal T3 and the antisense 5' *Mapk13* homology arm primer, to verify the correct orientation (expected product size was 1236bp, Figure 13). A colony containing a recombinant pEasyFusion-mCherry plasmid with correctly inserted 5' *Mapk13* homology arm was then sent for sequencing. A confirmed clone, containing the correctly modified pEasyFusion_mCherry plasmid (with both 5' and 3' *Mapk13* derived homology arms flanking the mCherry DNA) was then expanded (stored as a -80°C glycerol stock) and the correctly modified plasmid isolated (754.4ng/μl) and sequence verified.

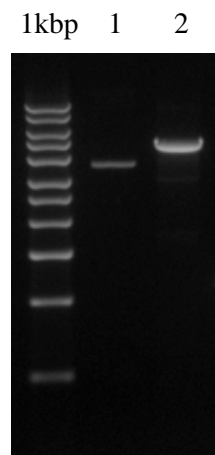


Figure 12. Gel electrophoresis showing linearized pEasyFusion_mCherry plasmid containing the digested empty pEasyFusion_mCherry plasmid (lane 1, 3663bp) and pEasyFusion_mCherry plasmid with 3' *Mapk13* homology arm (lane 2, 4739bp). A 1Kb ladder marker is shown for size reference (from top to bottom: 10, 8, 6, 5, 4, 3, 2.5, 2, 1.5, 1 & 0.5 Kb).

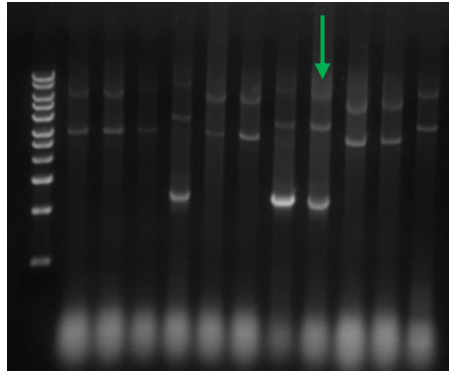


Figure 13. Agarose gel depicting colony PCR screening of pEasyFusion_mCherry plasmid (already containing the *Mapk13* specific 3' homology arm) containing clones for the successful insertion of the 5' homology arm of the *Mapk13* gene. Colony PCR was performed with T3 and *Mapk13* gene 5' homology arm antisense primer to indicate of a correct orientation of the cloned insert. The expected size was 1236bp (*i.e.* from the T3 primer till antisense primer of the 5' homology arm insert – highlighted by a green arrows, indicating individual clone sent for sequencing). A 1Kb ladder marker is shown for size reference (from top to bottom: 10, 8, 6, 5, 4.3, 2.5, 2, 1.5, 1 & 0.5 Kb).

4.1.1.3. *Mapk14* gene 5' and 3' homology arm cloning

To generate modified recombinant pEasyFusion_mCherry plasmid containing appropriately cloned 5' and 3' homology arms specific to the *Mapk14* genomic locus, an essentially similar strategy to that employed for the *Mapk13* specific inserts (as described above) was adopted. However, the empty pEasyFusion_mCherry plasmid was first digested with *EcoRI* in preparation to receive an *EcoRI* digested insert (corresponding to 5' homology arm of the *Mapk14* locus) rather than first using *BamHI* digest to clone the 3' homology arm of the *Mapk14* locus. Post-ligation and transformation, the obtained colonies were similarly screened in a 2-step colony PCR reaction. Firstly using the universal T7 and T3 primers (Figure 14, gel A - the expected PCR product size was 2140bp), and then with T3 and 5' *Mapk14* homology arm antisense primers (Figure 14, gel B – theorised PCR product size was 1336bp, confirming the correct orientation of the cloned insert). A confirmed clone was then expanded (stored as a -80°C glycerol stock) and the correctly modified plasmid isolated (371ng/μl) and sequence verified.

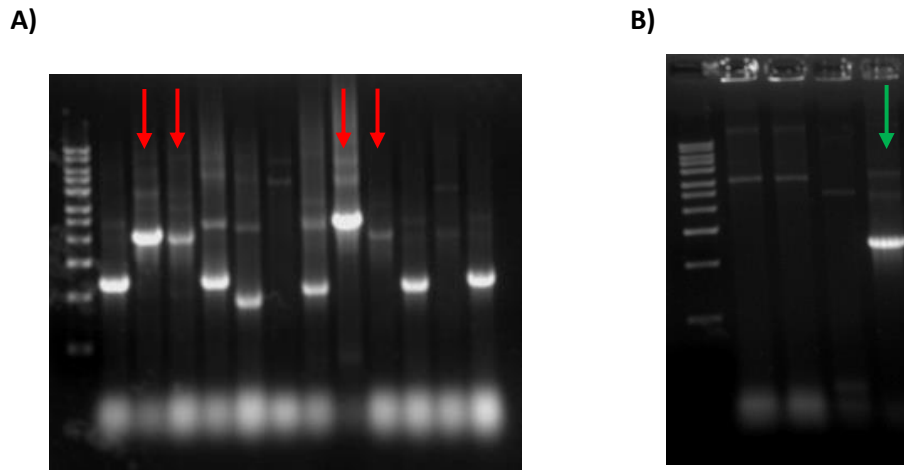


Figure 14. Agarose gels depicting 2-step colony PCR screening of pEasyFusion_mCherry containing clones for the successful insertion of the 5' homology arm of the *Mapk14* gene (highlighted with a red/green arrows). **A)** Colony PCR conducted with universal T3 and T7 primers that yield a 2113bp product if the insert is present (candidate clones highlighted by red arrows). **B)** Colony PCR performed with T3 and *Mapk14* gene 5' homology arm antisense primer to indicate of a correct orientation of the cloned insert. The expected size was 1336bp (*i.e.* from the T3 primer till the antisense primer of 5' homology arm insert, highlighted with green arrow). Subsequently, colony was taken for isolation and sequence verification. A 1Kb ladder marker is shown for size reference (from top to bottom: 10, 8, 6, 5, 4, 3, 2.5, 2, 1.5, 1 & 0.5 Kb).

After sequence confirmation, the pEasyFusion_mCherry plasmid containing the 5' *Mapk14* specific homology arm was linearized with *BamHI*, alkaline phosphatase treated and purified (143ng/μl – in preparation to receive the 3' *Mapk14* homology arm insert). Successful linearization was confirmed by resolving the digestion product on an agarose gel (alongside the empty pEasyFusion_mCherry vector- Figure 15) and the vector was subsequently ligated with the prepared *BamHI* digested 3' *Mapk14* homology arm insert. Post-transformation, bacterial colonies were again screened for successful insert incorporation, by 2-step colony PCR. Firstly, using the universal T3 and T7 primers (expected product size of 3250bp – *gel not show*) and then the positive colonies with T7 and the 3' *Mapk14* homology arm sense primer, to confirm correct insert orientation (Figure 16, expected PCR product size of 1206bp). The colony PCR confirmed clone was then expanded (stored as a -80°C glycerol stock) and the modified plasmid isolated (518.1ng/μl).



Figure 15. Gel electrophoresis showing linearized pEasyFusion_mCherry plasmid containing the 5' *Mapk14* homology arm (lane 1, 4921bp) or the empty pEasyFusion_mCherry plasmid (lane 2, 3663bp). A 1Kb ladder marker is shown for size reference (from top to bottom:10, 8, 6, 5, 4, 3, 2.5, 2, 1.5, 1 & 0.5 Kb).

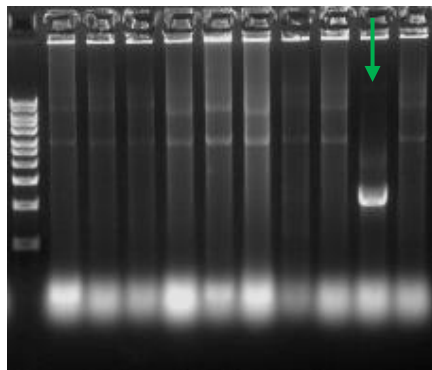


Figure 16. Agarose gel depicting colony PCR screening of pEasyFusion_mCherry plasmid (already containing the *Mapk14* specific 5' homology arm) containing clones for the successful insertion of the 3' homology arm of the *Mapk14* gene (indicated by the green arrow). Colony PCR performed with T7 and *Mapk14* gene 3' homology arm sense primer, the expected size (indicative of a correct orientation of the cloned insert) was 1206p (*i.e.* the size from the sense primer of 3' homology arm insert till T7 primer). The colony highlighted by a green arrow was isolated and sequence verified. A 1Kb ladder marker is shown for size reference (from top to bottom:10, 8, 6, 5, 4,3, 2.5, 2, 1.5, 1 & 0.5 Kb).

However, the sequencing results of the obtained clone confirmed from the colony PCR identified/verified a clone which comprised two distinct plasmid derived sequences, in the 5' *Mapk14* specific homology arm region. In the 5' homology arm, there was detected an additional 300bp section of non-*Mapk14* related sequence, that, when compared against the mouse genome, it was found to be derived from *Mapk11* gene and was embedded in the

Mapk14 derived sequence. The origin of this embedded *Mapk11* derived sequence, within the correct *Mapk14* specific 5' homology arm sequence is not clear. However, if plasmid derived from this clone was PCR amplified using universal T3 and *Mapk14* gene 5' homology arm antisense primers, two PCR products could be observed (one of the correct/anticipated 1258bp and another ~300bp larger in sequence, thus confirming the presence of plasmid sequence with and without the spurious *Mapk11* sequence (Figure 17). It is possible this could have arisen as the consequence of inadvertently picking up two colonies, however, as the plasmid clone is needed to derive *Mapk14* specific biotinylated dsDNA HDR template (via a subsequent BIO-PCR protocol) it was not possible to use this clone.

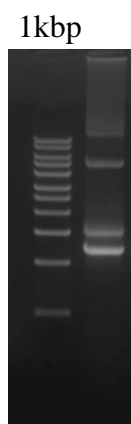


Figure 17. PCR amplification of the colony PCR identified recombinant pEasyFusion_mCherry plasmid clone containing both 5' and 3' *Mapk14* specific homology arms using universal T3 and *Mapk14* gene 5' homology arm antisense primers. The generation of bands of the correct/anticipated size (1336bp) and of the theorised size +300bp, confirms the presence of two plasmid species in the clone. A 1Kb ladder marker is shown for size reference (from top to bottom:10, 8, 6, 5, 4,3, 2,5, 2, 1,5, 1 & 0,5 Kb).

Therefore, to try and mitigate this problem, the plasmid preparation was retransformed, and fresh individual colonies were selected and screened using colony PCR to identify the size of the derived troublesome 5' *Mapk14* homology arms. In all cases (*gels not shown*) both the correct and +300bp products were obtained. Therefore, it was decided to repeat the whole cloning procedure for inserting both the 5' and 3' *Mapk14* specific homology arms (beginning with the troublesome 5' homology arm). Whilst, in this second attempt, the 5' *Mapk14* homology arm was successfully cloned and sequence verified, a new problem arose with the insertion of the 3' *Mapk14* homology arm (typified by the presence of a ~150bp of non-specific sequence). Owing to time constraints, it was decided the original clone (comprising both appropriate and +300bp *Mapk11* sequence) would be taken forward for BIO-PCR based

generation of the *Mapk14* specific biotinylated dsDNA HDR template, as the product size could be later scrutinised. If it were not suitable, a decision not to microinject it into mouse embryo blastomeres could be taken then.

4.1.2. Production of target gene specific biotinylated dsDNA HDR templates

The recombinant pEasyFusion_mCherry vectors, containing the cloned inserts of the 5' and 3' homology arms (flanking the mCherry cDNA sequence – *described above*) of the candidate/target genes, were used as template in BIO-PCR reactions. It was performed to generate the required biotinylated dsDNA HDR templates needed for mouse embryo blastomere microinjection (as part of the planned *in situ* genome editing). The BIO-PCR reaction employed pEasyFusion_mCherry vector specific universal primer sites to amplify the entire dsDNA HDR template region (*i.e.* 5' homology arm- mCherry cDNA- 3' homology arm) using oligos with 5'-biotin conjugates. Firstly, the derived products were purified by phenol-chloroform extraction, ethanol precipitated, and after resuspension their expected sizes were confirmed by agarose gel electrophoresis (Figure 18 – BIO-PCR products relating to the generation of dsDNA HDR templates for the *Wwc2* and *Mapk13* genes) and found to be correct.

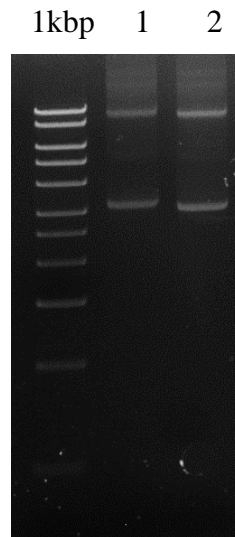


Figure 18. Agarose gel showing BIO-PCR products for the generation of biotinylated dsDNA HDR templates for (1) the *Wwc2* gene, with an expected product size of 3161 bp, and (2) the *Mapk13* gene, with a product size 3069bp. A 1Kb ladder marker is shown for size reference (from top to bottom: 10, 8, 6, 5, 4.3, 2.5, 2, 1.5, 1 & 0.5 Kb).

However, as observed in the agarose gels (Figure 18) high molecular weight DNA was also observed. It was hypothesised that this may reflect template recombinant pEasyFusion_mCherry plasmid DNA. Therefore, the purified BIO-PCR products were digested with the restriction enzyme *DpnI* (to remove methylated plasmid DNA but not digest non-methylated PCR product) for 1 hour or overnight. The *DpnI* restriction digestion products were then ran on an agarose gel (Figure 19). However, this did not result in the removal of the high molecular weight DNA.

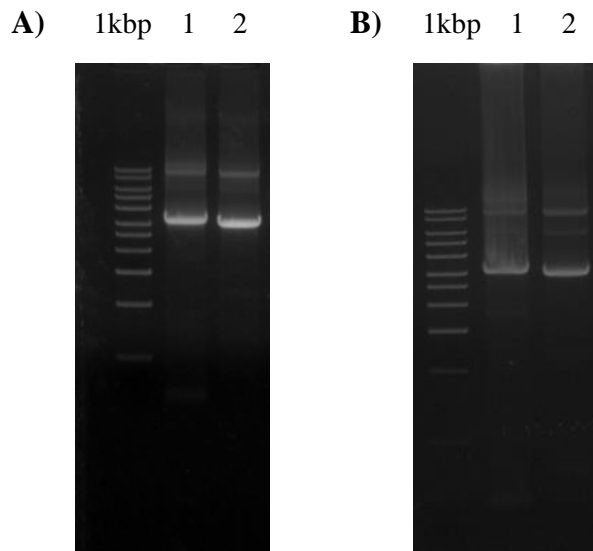


Figure 19. Agarose gel electrophoresis of *DpnI* digested BIO-PCR products for the generation of *Wwc2* (left, expected product size 3161bp) and *Mapk13* (right, expected product size 3069bp) biotinylated dsDNA HDR templates: (A) 1 hour or (B) overnight *DpnI* digests. A 1Kb ladder marker is shown for size reference (from top to bottom:10, 8, 6, 5, 4,3, 2.5, 2, 1.5, 1 & 0.5 Kb).

Therefore, in a second attempt to only obtain one specific BIO-PCR band (*i.e.* the gene-specific biotinylated dsDNA HDR templates), a gel extraction strategy was employed on freshly prepared BIO-PCR products (focussing on those derived from amplification of the *Mapk14* homology arm containing clone comprising the two identified sequences, as a prove of principle). Accordingly, the *Mapk14* BIO-PCR band corresponding to the correct/appropriate size was extracted from an excised gel slice and the resulting DNA re-used as template in a repeat BIO-PCR reaction. However, after this second round of BIO-PCR using gel extracted template, the expected product was not obtained, possibly due to unfavourable ionic conditions in the template preparation after gel extraction (Figure 20). Hence, it was

decided not to extend this approach to the *Wwc2* and *Mapk13* specific BIO-PCR products and to solely focus on generating biotinylated dsDNA HDR templates for these two genes.

1kbp Product

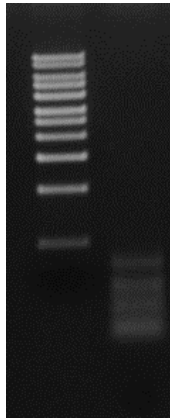


Figure 20. Agarose gel electrophoresis of the second round of BIO-PCR reactions, specific for the *Mapk14* gene. After first gel extracting template or the correct size. A 1Kb ladder marker is shown for size reference (from top to bottom:10, 8, 6, 5, 4,3, 2.5, 2, 1.5, 1 & 0.5 Kb).

Ultimately, it was decided to repeat the original BIO-PCR but using a low template concentration (10ng/ μ l) and not to purify the products using the previously adopted phenol-chloroform based protocol (as this favours the isolation of high molecular weight DNA and has the potential to damage the biotin-conjugates at the 5' ends of derived PCR products). Therefore, the newly synthesised BIO-PCR products were purified using a QIAquick PCR purification kit (from Qiagen), followed by ethanol precipitation of the eluate and final resuspension of DNA pellets in HPLC grade water (to final concentrations of 248.3 ng/ μ l and 274.3ng/ μ l for *Wwc2* and *Mapk13* specific biotinylated dsDNA HDR templates, respectively). The correct size of these constructs was confirmed by agarose gel electrophoresis (Figure 21). These biotinylated dsDNA HDR templates were carried forward preimplantation mouse embryo blastomere microinjection.

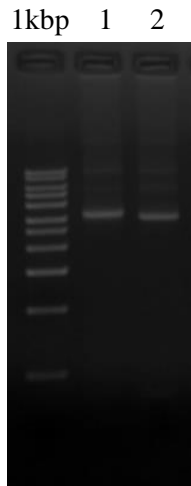
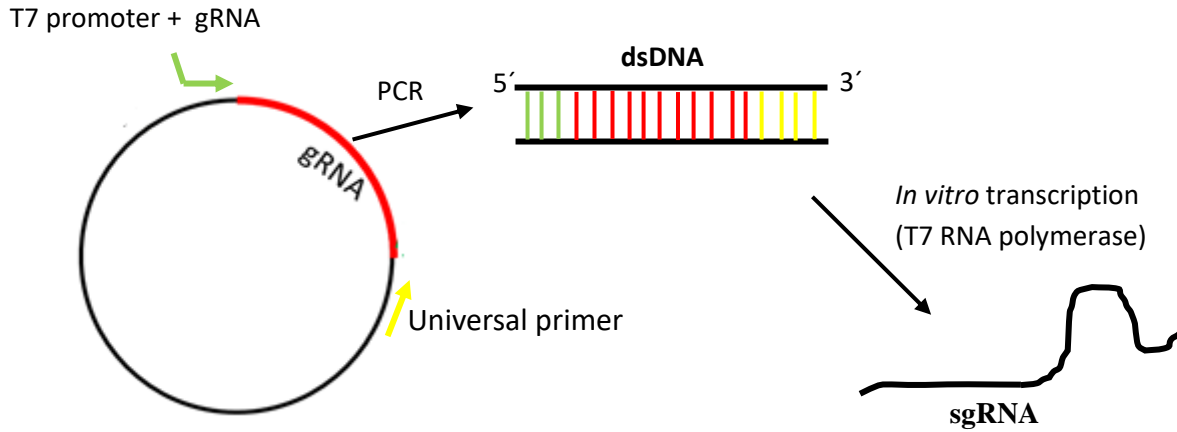


Figure 21. Final BIO-PCR products/ biotinylated dsDNA HDR templates specific for the *Wwc2* gene (lane 1, expected product size 3161bp) and the *Mapk13* gene (lane 2, expected product size 3069bp) used for microinjection into the preimplantation mouse embryo blastomeres. A 1Kb ladder marker is shown for size reference (from top to bottom:10, 8, 6, 5, 4,3, 2.5, 2, 1.5, 1 & 0.5 Kb).

4.2. Generation of gene sequence specific sgRNAs (*Wwc2*, *Mapk13* and *Mapk14*)

The second of the three required CRISPR-Cas9 mediated genome editing constructs (needed to fluorescently tag the endogenous target gene loci in microinjected preimplantation mouse embryo blastomeres) were the gene sequence specific sgRNAs (required to direct the Cas9 protein to the target gene loci). Therefore, according to this project's aims, specific sgRNAs for the three targeted genes (*i.e.* *Wwc2*, *Mapk13* and *Mapk14*) were prepared for eventual mouse embryo blastomere microinjection (*i.e.* together with gene specific biotinylated dsDNA HDR template and streptavidin-Cas9 mRNA). This strategy involved annealing 24 nucleotide long single stranded oligos (with homology to the targeted genomic loci – *i.e.* around the STOP codon of the last exon and proximal to the consensus PAM sequence) and then cloning them (by means of 5'-overhangs generated by the annealing process) into a suitable vector (in this case the plasmid pX330-U6-Chimeric_BB-CBh-hSpCas9). From such verified recombinant plasmid, a PCR product could then be derived containing a 5' located T7-RNA polymerase promoter followed by the target gene specific sequence and a tracrRNA-like encoding component (*i.e.* reconstituting the gene specific sgRNA sequence). Thereafter, it could be utilised in IVT to derive target gene specific sgRNA for embryo blastomere microinjection (see Figure 22). Note, that prior to my arrival in the laboratory, *Wwc2* gene specific annealed oligos had already been successfully ligated into the

pX330-U6-Chimeric_BB-CBh-hSpCas9 vector and sequence verified (by Federica Serati). Therefore, I just concentrated on generating the equivalent constructs for the *Mapk13* and *Mapk14* genes.



pX330-U6-Chimeric_BB-CBh-hSpCas9

Figure 22. The visualization of the generation sgRNA.

To generate target sgRNA (*i.e.* the direction of Cas9 to the proper place), 24bp complementary pairs oligos were annealed and cloned into pX330-U6-Chimeric_BB-CBh-hSpCas9 plasmid (see appendix, Figure 34). Subsequently, T7 polymerase promoter sequence was incorporated at the 5' end and PCR reaction was performed (sense primer partially composed of T7 polymerase sequence + other half of gRNA, and antisense universal primer complementary to the plasmid backbone) to produce dsDNA product. PCR product (*i.e.* dsDNA) was *in vitro* translated into sgRNA and subsequently (together with two other components *i.e.* mSA-Cas9 mRNA and biotinylated HDR repair template) co-microinjected into individual mouse blastomere.

4.2.1. Cloning of gene-specific oligos (*Mapk13* and *Mapk14*) into pX330-U6-Chimeric_BB-CBh-hSpCas9 plasmid

Firstly, it was necessary to linearize the pX330-U6-Chimeric_BB-CBh-hSpCas9 plasmid to accept the annealed oligo inserts. Extracted plasmid (477.7ng/ μ l) was digested with *BbsI* restriction enzyme in two adjacent recognition sequences in the vector. This ensured the generation of plasmid overhangs that were complementary to the 5' overhangs of the annealed oligos and also ensured the annealed oligos could only be inserted in the correct/appropriate orientation. In this case, the alkaline phosphatase treatment of the digested vector was not necessary as the generated plasmid overhangs flanking the digestion sites were not compatible with each other. Post-digestion the purified plasmid (265.1ng/ μ l) integrity and linearize size were checked/confirmed by agarose gel electrophoresis (the anticipated size being 8484bp, Figure 23).

1kbp uncut cut

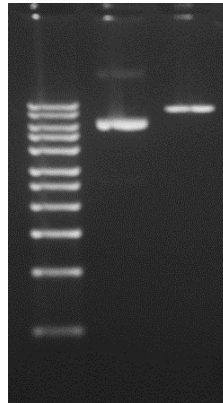


Figure 23. Agarose gel showing the pX330-U6-Chimeric_BB-CBh-hSpCas9 plasmid vector before (lane 1) and after digestion (with *BbsI*, lane 2). There is visible a significant difference between circular and linearized plasmid (with an expected size of 8484bp). A 1Kb ladder marker is shown for size reference (from top to bottom:10, 8, 6, 5, 4,3, 2.5, 2, 1.5, 1 & 0.5 Kb).

Confirmed annealed oligos (see Figure 24), specific for the *Mapk13* and *Mapk14* genes, were ligated with purified and restriction enzyme linearized (*BbsI*) pX330-U6-Chimeric_BB-CBh-hSpCas9 plasmid. Post bacterial transformation, the few colonies that appeared on LB agar plates were processed or colony PCR to identify clones containing successfully ligated plasmid with the gene-specific insert/oligos, using universal PCR primers (complementary to sequences in the plasmid backbone, section 3.2.1., Table XVI). The expected PCR product size, indicative of successful annealed oligo cloning, was 448bp (*i.e.* 24bp larger than the empty vector itself). Figure 25 shows an electrophoreses of a 2% agarose gel of colony PCR products obtained for *Mapk13* and *Mapk14* oligo specific ligations.

100bp 1* A S 2* A S

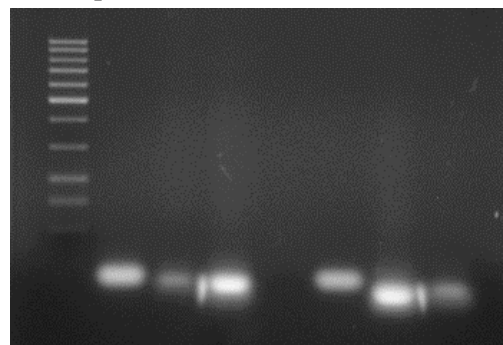


Figure 24. Annealed oligos specific for the targeted *Mapk13* (1* - left) and *Mapk14* (2* - right) genomic loci and their constituent single stranded counterparts (A = antisense oligo strand and S = sense oligos strand) were electrophoresed alongside each other in 2% agarose gels, to confirm successful complementary oligo annealing. The concentrations of annealed oligos were 47.5 ng/ μ l (*Mapk13*) and 54.5 ng/ μ l (*Mapk14*). Note, the retarded mobility of the

annealed oligos compared to the single stranded oligos, denoting successful annealing. A 100bp ladder marker is shown for size reference (from top to bottom: 1000, 900, 800, 700, 600, 500, 400, 300, 200, 150 & 100 bp).

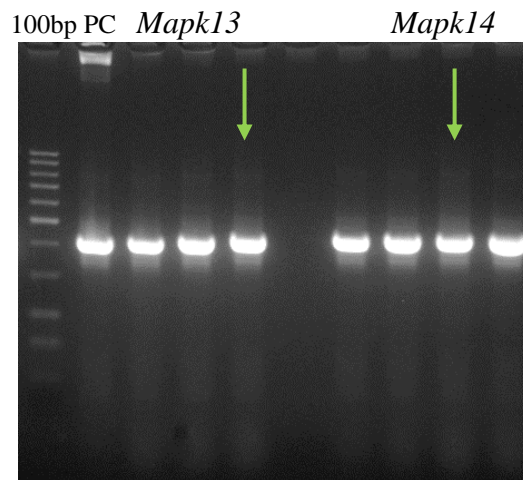


Figure 25. 2% agarose gel of resolved colony PCR products arising from ligating/cloning *Mapk13* (left) and *Mapk14* (right) target genomic sequence specific annealed oligos into the pX330-U6-Chimeric_BB-CBh-hSpCas9 vector. Universal primers are complementary to plasmid backbone providing PCR product (428bp- not cloned insert vs 448bp with insert cloned). Colonies highlighted with the green arrows indicate candidate clones for successful insert integration (used for the sequence verification). A PCR positive control (PC) condition using the same universal primers (complementary to vector backbone) and undigested pX330-U6-Chimeric_BB-CBh-hSpCas9 vector as template (*i.e.* expecting size 428bp) was included (lane 1). A 100bp ladder marker is shown for size reference (from top to bottom: 1000, 900, 800, 700, 600, 500, 400, 300, 200, 150 & 100 bp).

4.2.2. Generation of single guides RNAs (for *Wwc2*, *Mapk13* and *Mapk14*) prepared for the microinjection

The purified and sequence verified recombinant pX330-U6-Chimeric_BB-CBh-hSpCas9 plasmids (containing the newly derived *Mapk13* and *Mapk14* gene-specific oligo inserts, plus the originally derived *Wwc2* specific construct) were then used as templates in PCR reactions to generate PCR products from which the gene specific sgRNA constructs could be transcribed (by IVT). The utilised sense primers all contained 5' proximal T7-RNA polymerase promoter sequence, followed by sequence specific to the target gene specific cloned oligo. The antisense PCR primer was by contrast universal and complementary to sequence in the vector backbone. The resulting PCR products were resolved on a 2% agarose gel and had an expected/predicted size of 120bp (Figure 26).

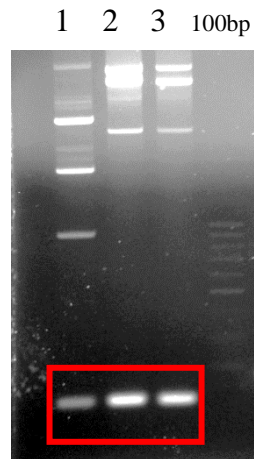


Figure 26. Agarose gel of resolved PCR products arising from amplification of recombinant pX330-U6-Chimeric_BB-CBh-hSpCas9 cloned inserts, corresponding to target gene specific sgRNA encoding sequence (anticipated size, 120bp – see products highlighted with the red box). From left to right, (1) *Wwc2*, (2) *Mapk13* and (3) *Mapk14*. A 100bp ladder marker is shown for size reference (from top to bottom: 1000, 900, 800, 700, 600, 500, 400, 300, 200, 150 & 100 bp).

Although T7-RNA-polymerase promoter-linked PCR products, of the appropriate size, were obtained for each target gene specific sgRNA encoding variant, it was clear the reactions also contained some high molecular weight DNAs (most probably related to the plasmid DNA used as template in the PCR reaction). Therefore, excised gel slices containing the correctly sized 120bp PCR product were gel extracted, ethanol precipitated and resuspended in HPLC grade water (obtained sgRNA template DNA concentrations: *Wwc2* specific, 20.7ng/ μ l, *Mapk13* specific, 54ng/ μ l and *Mapk14* specific, 26.7ng/ μ l). The integrity of these isolated/purified PCR products was again confirmed by electrophoresis on 2% agarose gels (Figure 27).

100bp 1 2 3

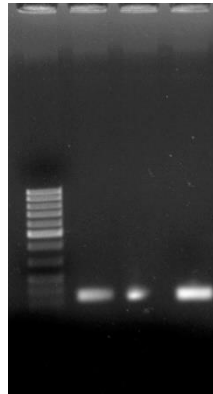


Figure 27. Agarose gel showing gel extracted and target gene-specific sgRNA PCR derived templates (incorporating 5' proximal T7-RNA polymerase promoter sequence). (1) *Wwc2* specific, (2) *Mapk13* specific and (3) *Mapk14* specific. A 100bp ladder marker is shown for size reference (from top to bottom: 1000, 900, 800, 700, 600, 500, 400, 300, 200, 150 & 100 bp).

These obtained, target gene specific and T7-RNA polymerase promoter containing sgRNA encoding PCR products were subsequently used as template in IVT reactions (using MEGAscript™ T7 transcription kit). The generated sgRNA transcripts were then purified by conventional phenol-chloroform extraction and overnight precipitation in isopropanol. The resulting purified sgRNA pellets were then resuspended and the derived yield (and purity) assessed by UV spectrophotometry (obtained sgRNA concentrations: *Wwc2* specific sgRNA, 1273ng/μl, *Mapk13* specific sgRNA, 2154.5ng/μl and *Mapk14* specific sgRNA:1395.3ng/μl). Target gene specific sgRNAs integrity was confirmed by agarose gel electrophoresis under denaturing conditions (as the sgRNA constructs are single stranded and by their nature and form regular secondary structures by intra-molecular base-pair specific hydrogen bonding; expected sgRNA length = 120bp, Figure 28). These derived target gene specific sgRNA transcripts were taken forward to preimplantation mouse embryo blastomere microinjection (to attempt to elicit the desired genome editing).

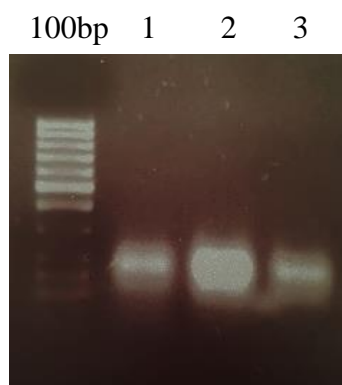


Figure 28. Agarose gel, electrophoresed in denaturing conditions (to ensure extended single stranded confirmation of sample and markers), of IVT derived sgRNA transcripts specific for (1) *Wwc2*, (2) *Mapk13* and (3) *Mapk14* genes (expected transcript size, 120bp). A 100bp ladder marker is shown for size reference (from top to bottom: 1000, 900, 800, 700, 600, 500, 400, 300, 200, 150 & 100 bp).

4.3. Generation of Cas9-streptavidin mRNA

The third and final component required for the intended *in situ* CRISPR-Cas9 mediated genome editing of preimplantation stage mouse blastomeres was the generation of streptavidin-Cas9 encoding mRNA (*i.e.* to be microinjected with the other two derived and target gene specific components – biotinylated dsDNA HDR template and sgRNA, *see above*). This was achieved utilising the plasmid pCS2⁺-Cas9-mSA (that includes the Cas9 coding sequence, from *Streptococcus pyrogens*, C-terminally fused in-frame with cDNA encoding monomeric streptavidin/mSA and has a total size of 8883bp). Isolated and purified plasmid (the concentration 488.1ng/μl) was linearized by *NotI* restriction enzyme digest (confirmed by agarose gel electrophoresis, Figure 29) and subsequently used (after phenol-chloroform and ethanol precipitation purification) as template in IVT (utilising the plasmid encoded SP6-RNA polymerase promoter). Post-IVT, the derived Cas9-mSA mRNA transcript was polyadenylated (*i.e.* the addition of a poly-A tail) and electrophoresed on a denaturing agarose gel alongside an aliquot of the non-polyadenylated mRNA (Figure 30). The polyadenylated Cas9-mSA mRNA was then immediately ethanol precipitated, resuspended in HPLC water and quantified by UV spectrophotometry (concentration, 675ng/μl), before being stored at -80°C as aliquots until needed for preimplantation mouse embryo blastomere microinjection.

1kbp cut uncut

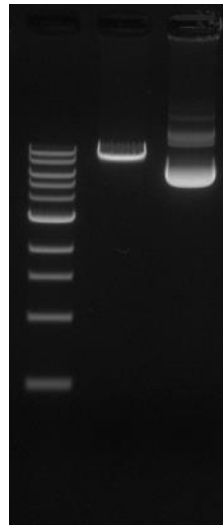


Figure 29. Agarose gel electrophoresis *NotI* digested/linearized (lane 1) and non-digested (lane 2) pCS2⁺-Cas9-mSA plasmid (8883bp). The differing electrophoretic mobility of the two lanes, confirms the successful linearization of the pCS2⁺-Cas9-mSA plasmid by *NotI*. A 1Kb ladder marker is shown for size reference (from top to bottom:10, 8, 6, 5, 4, 3, 2, 1.5, 1 & 0.5 Kb).

1kbp mRNA mRNA
+
polyA end

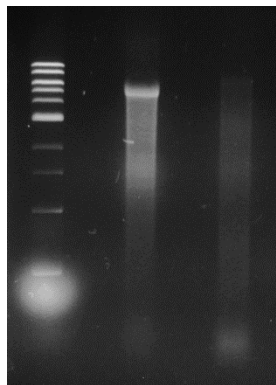


Figure 30. Denaturing agarose gel electrophoresis of IVT derived Cas9-mSA encoding mRNA before (left, lane 2) and after polyadenylation/poly-A tailing (right, lane 4). The expected size of mRNA was 4818bp. A 1Kb ladder marker is shown for size reference (from top to bottom:10, 8, 6, 5, 4, 3, 2, 1.5, 1 & 0.5 Kb).

4.4. Assaying fluorescent mCherry-tagged endogenous gene expression (*i.e.* *Wwc2*, *Mapk13*) in peri-implantation mouse embryo blastomeres

Following the successful construction of all three CRISPR-Cas9 reagents (*i.e.* target gene specific sgRNA and biotinylated dsDNAs HDR template, plus Cas9-mSA mRNA), they were microinjected into individual 2-cell stage embryo blastomeres. The microinjection procedure itself was independently performed by a skilled and trained Ph.D. student in the laboratory (Rebecca Collier, as presented here and continued by Giorgio Virnicchi). Due to time constraints (in the context of this thesis), the microinjections reported only targeted the *Wwc2* and *Mapk13* genes (*i.e.* as described above, there were some concerns relating to the generation of biotinylated dsDNA HDR template specific for the *Mapk14* gene). A strategy of microinjecting into only one of the two blastomeres of late 2-cell stage preimplantation mouse embryos was adopted. This would create a clone of potentially genome edited progeny cells. Potentially expressing fluorescent mCherry fusions of the targeted gene proteins of interest would collectively represent 50% of the total cell number of individually microinjected embryos. Therefore, in theory, the potential mCherry fluorescent signal indicative of successful genome editing that could be internally compared between the progeny of both the originally microinjected and non-microinjected 2-cell stage blastomeres. Accordingly, a series of experimental microinjections, in which various parameters relating to the relative concentration of the microinjected CRISPR-Cas9 reagents were varied (after first assaying for the expression of mCherry derived fluorescence), were undertaken and are summarised in table XXIII. In most cases, an additional IVT derived mRNA encoding a fluorescent marker, *e.g.* plasma membrane localised GAP43-GFP or cytoplasmic/soluble EGFP, was co-microinjected to aid identification of the microinjected clone (experimental conditions 1-5, although in latter case this was omitted, experimental condition 6). Moreover, under the later microinjection experimental conditions (4-6), embryos were subsequently *in vitro* culture in KSOM culture media without exogenous amino-acid supplementation, as it was thought this may elicit enhanced expression of the, potentially edited, *Mapk13* stress-kinase locus.

Table XXIII: A summary of the varying components concentrations of target gene specific CRISPR-Cas9 genome editing reagents microinjected into single blastomeres of 2-cell stage preimplantation mouse embryo and their subsequent *in vitro* culture conditions. Note, the CRISPR-Cas9 construct concentrations highlighted in grey represent those that were used in the paper of Gu *et al.*, 2018 (the report that first described successful genome editing to created fluorescent reporter fusions of endogenously expressed genes in mouse preimplantation embryos).

Exp.	Assayed developmental stage (mCherry expression)	KSOM with (+), without (-) amino acids	Gene	Injection marker (mRNA)	Concentrations			
					sgRNA (ng/ μ l)	Cas9-mSA mRNA (ng/ μ l)	Biotinylated dsDNA HDR template (ng/ μ l)	Injection marker (ng/ μ l)
1	E3.5	+	<i>Mapk13</i>	GAP43-GFP	75	112	30	60
2	E3.5	+	<i>Mapk13</i>	GAP43-GFP	50	75	20	60
3	E3.5	+	<i>Mapk13</i>	GAP43-GFP	37.5	56	15	60
4	E4.25	-	<i>Mapk13</i>	GAP43-GFP	50	75	20	60
5	E2.5	-	<i>Wwc2</i>	EGFP	50	75	20	60
6	E4.25	-	<i>Mapk13</i>	none	50	75	20	60

In all the cases summarised in table XXIII, microinjected 2-cell stage embryos were *in vitro* cultured to an appropriate and indicated developmental stage. Afterwards, they were assayed for evidence of mCherry fluorescence (using confocal microscopy of fixed embryo preparations) indicative of successful target genome editing. Moreover, potentially providing/revealing information on the sub-cellular localisation of the mCherry-tagged target protein and/or potential lineage restricted expression (particularly in blastocyst embryos assayed at E3.5 and beyond). As an experimental baseline, embryos were usually microinjected with CRISPR-Cas9 specific constructs at the same concentration previously reported by Gu and colleagues. Their original paper describes the first successful CRISPR-Cas9 mediated genome editing in embryos resulting in fluorescently tagged/fusion-endogenous gene reporters (Gu *et al.*, 2018) (highlighted in grey, in Table XXIII). When targeting the *Mapk13* gene, the concentrations were modified (Table XXIII, experimental conditions 1 and 3) to microinject more or less of the prepared CRISPR-Cas9 constructs. Also,

in the case of targeting the *Mapk13* gene, we initially assayed for mCherry expression at E3.5 (Table XXIII, experimental conditions 1, 2 and 3), given the previous data from our reports indicating a functionally important role of p38-MAPKs during blastocyst maturation (E3.5-E4.5) and PrE specification/differentiation. Additionally, we assayed a time-point that represented a more advanced developmental point in the mouse blastocyst (*i.e.* E4.25 - Table XXIII, experimental conditions 4 and 6). In regard to targeting of the *Wwc2* gene, we initially chose the E2.5 developmental time-point because it is equivalent to the 8-cell stage and our previous data revealed blastomere cell division defects beginning at the 8- to 16-cell stage transition (Virnicchi *et al.*, 2020) (Table XXIII, experimental condition 5).

Unfortunately, despite microinjecting the *Wwc2* and *Mapk3* specific CRSIPR-Cas9 constructs under such varied conditions (within the last few weeks of my experimental work) we were not able to unequivocally confirm any mCherry fluorescent protein expression potentially indicative of the successful genome editing. Indeed, we found no evidence of mCherry expression in the embryos of experimental conditions 1-5 (described in Table XXIII). This was despite being able to observe the clonal progeny of successfully microinjected 2-cell stage embryos, revealed by plasma-membrane localised GAP43-GFP fluorescence (Figure 31, exemplar single z-stack confocal micrographs, relating to experimental condition 4, targeting gene *Mapk13* and assayed at developmental stage E4.25). Whilst, this was disappointing, it may reflect a simple need to optimise the microinjection conditions and the concentration of microinjected CRISPR-Cas9 reagents (as the volumes of microinjected material can vary greatly from individual experimenter and from laboratory to laboratory). However, in experimental condition 6 (Table XXIII), targeting the *Mapk13* gene (using previously published concentrations of CRISPR-Cas9 reagents, without a fluorescent co-microinjected marker mRNA and *in vitro* culture in media without amino-acid supplementation) we did observe some limited red fluorescence that could be compatible with mCherry expression from an edited genome (see example E4.25 stage blastocyst, single z-stack confocal micrographs- Figure 32).

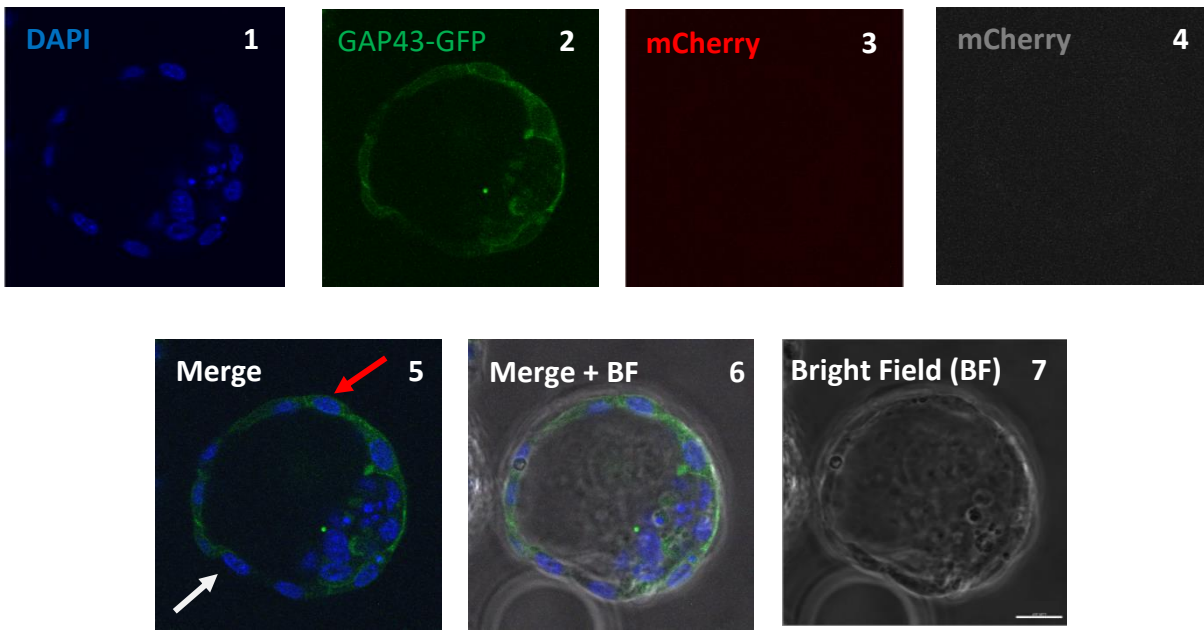


Figure 31. Single z-stack confocal micrographs of a *Mapk13* gene specific CRISPR-Cas9 construct microinjected mouse embryo, with the injection marker (Gap43-GFP, a protein expressed in the cytoplasm), fixed at the E4.25 blastocyst stage (microinjected in a single 2-cell stage blastomere). Panel 1 shows the DNA DAPI counterstained channel (blue), panel 2 shows the injection marker (GAP43-GFP) specific panel. Panels 3 and 4 show the mCherry specific channel in red and in a grey-scale version, respectively. Panel 5 and panel 6 show merges of the DAPI and mCherry (red) channels and the same including a merge of the bright field channel, respectively. Panel 7 shows the bright field channel alone (allowing visualisation of the area of the blastocyst cavity and ICM). In panel 5, the white arrow denotes a cell originally derived from non-injected 2-cell stage clone, whereas the red arrow highlights a cell derived from the microinjected 2-cell stage clone (confirming successful reagent microinjection). The scale bars represent 20µm.

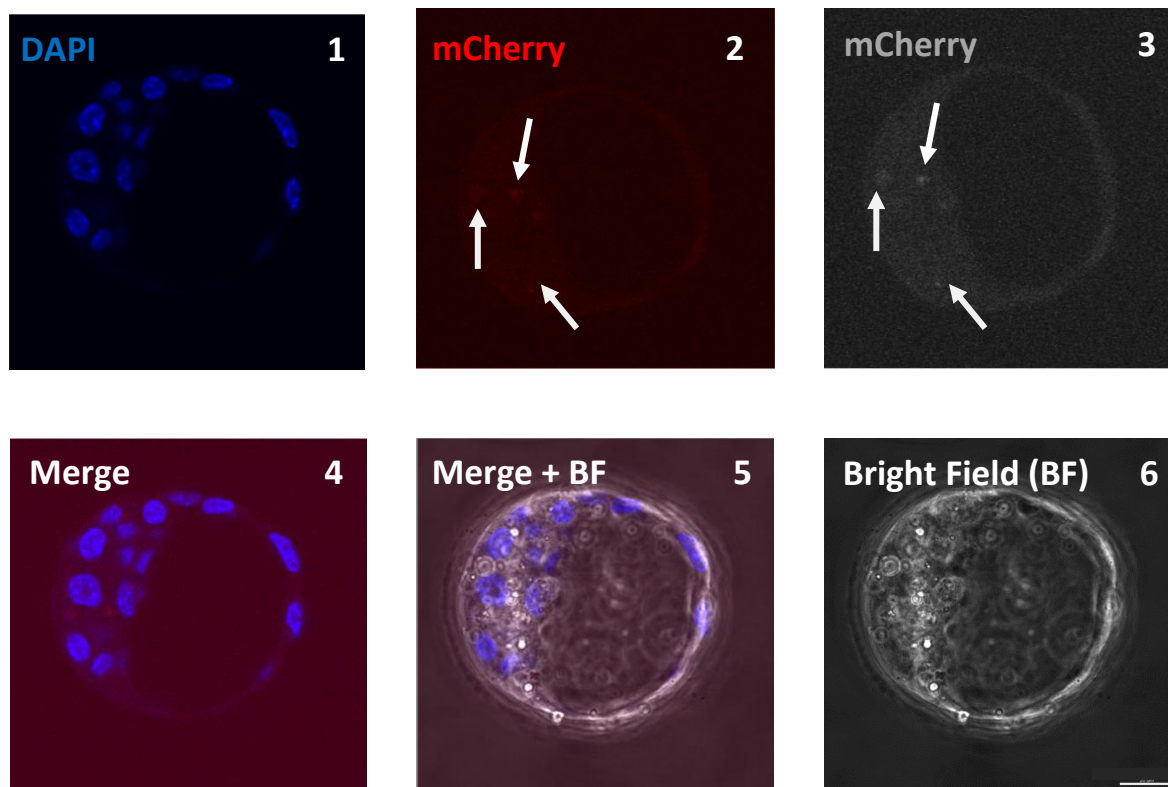


Figure 32. Exemplar, single z-stack confocal micrographs of a *Mapk13* gene specific CRISPR-Cas9 construct microinjected and fixed E4.25 stage mouse blastocyst embryo (microinjected in a single 2-cell stage blastomere) showing potential, but limited, mCherry expression (potentially indicative of endogenous *Mapk13*-mCherry fusion gene protein expression, after successful genome editing – highlighted with white arrows, panels 2 and 3). Panel 1 shows the DNA DAPI counterstained channel (blue), panel 2 shows the mCherry specific channel (red) while panel 3 shows the mCherry specific channel but in a grey-scale version (to aid visualisation of mCherry expression). Panel 4 and panel 5 show merges of the DAPI and mCherry (red) channels and the same including a merge of the bright field channel, respectively. Panel 6 shows the bright field channel alone (allowing visualisation of the area of the blastocyst cavity and ICM). The scale bar represents 20 μ m.

Despite not being able to obtain clear mCherry expression after these first few recorded preimplantation mouse embryo blastomere microinjection attempts, reported within this thesis, the work conducted to this point nevertheless provides a useful baseline for the future and on-going microinjections by other members of the laboratory. With continued optimisation (*e.g.* changing the concentrations of individual CRISPR-Cas9 reagents, preparing fresh microinjection reagents from already derived plasmid constructs and/or assaying at different developmental time points) we are confident the technique can be made to reliably work.

5. Discussion

The principle aim of this Master's thesis was to generate the required CRISPR-Cas9 constructs and reagents needed to effect *in situ* genome editing and create fluorescent mCherry reporter fusions of the endogenous *Wwc2*, *Mapk13* and *Mapk14* genes. Secondly, if time permitted, to utilise these reagents in single/individual preimplantation mouse embryo blastomere microinjections and to create mosaic clones of such genome edited cells that could impart temporal and spatial expression information about these genes targeted during early embryogenesis. In this thesis, I have described the complete satisfaction of the first aim in relation to the *Wwc2* and *Mapk13* genes (plus near completion of the *Mapk14* related constructs with the exception of the troublesome 5' homology arm required to generate the biotinylated dsDNA HDR template) and presented initial experimental data relating to the second aim that is currently being optimised by other members of the group.

As referenced elsewhere in this thesis, successful preimplantation mouse embryo blastomere *in situ* genome editing leading to the incorporation of C-terminally fluorescent tags in place of the STOP codons of endogenous genes has already been described (confirmed by the expression of several fluorescent mCherry-endogenous fusion gene proteins in blastocysts *e.g.* *Cdx2* in TE, *Nanog* in EPI and *Gata4* in PrE - Gu *et al.*, 2018). Indeed, expression was detected in both live (compatible with fluorescence time-lapse microscopy and bringing an extra level of refinement to measuring the temporal expression of candidate genes of interest) and fixed embryos samples. In this thesis, we have tried to remain as faithful to the methods described in this study as possible. For example, microinjecting the derived CRISPR-Cas9 reagents at the same concentrations and at the same late S-G2 phase of the cell cycle in individual 2-cell stage preimplantation mouse embryos shown to be the most efficient stage for successful genome editing (Gu *et al.*, 2018). However, we are still in the early stages of optimizing the protocol and need to explore varying some of the parameters regarding microinjection. Specifically, the concentration of the CRISPR-Cas9 reagents, as it is not possible to standardise the exact microinjection volumes achieved between different laboratories or indeed by individual researchers, thus, requiring an empirical approach to optimisation.

As the bulk of the described results relate to somewhat conventional molecular biology (that was largely successfully achieved, including necessary optimisation, and troubleshooting as required), I will use this Discussion section to expand upon the potential usefulness of

successfully deriving mCherry fusion reporters of targeted endogenous genes, by *in situ* CRISPR-Cas9 mediated genome editing in preimplantation mouse embryos rather than discussing routine molecular biology related themes.

The creation of CRISPR-Cas9 mediated (*i.e.* genome edited) C-terminal mCherry fluorescent fusions with endogenous genes has the potential to serve as a faithful marker/reporter of the targeted gene's expression. In the case of preimplantation mouse embryos, the detection of mCherry reporter fluorescence by confocal microscopy can help characterise the temporal expression of the targeted gene throughout the preimplantation developmental period. Potentially, highlighting specific developmental windows in which the gene is expressed (for example, potentially associated with key morphological changes such as embryo compaction, blastomere polarisation or blastocyst cavity formation). Moreover, it can additionally impart spatial embryonic expression data reporting in which specific cells the gene of interest is translated (for example, being specifically limited to one of the three late blastocyst lineages *i.e.* TE, PrE and EPI). Thus, by integrating such temporal and spatial mCherry derived reporter expression data, it is possible to create and experimentally test novel hypotheses related to the targeted gene of interest (*i.e.* as is the underlying intention in targeting the *Wwc2*, *Mapk13* and *Mapk14* genes in this thesis project). Furthermore, because the generated mCherry reporter is a fusion protein with the endogenous gene of interest, we can gain information on the sub-cellular localisation of the targeted protein that could again inform its function (*e.g.* if it is localised to the plasma membrane, nucleus or specific organelle or a potentially transient structure such as the mitotic spindle apparatus). Additionally, the genome editing mediated creation of such reporter fusions with endogenous genes has the advantage that all the normal gene regulatory mechanisms which govern the expression of the unmodified gene (*e.g.* specific transcription factor mediated regulation of transcription of the targeted gene genomic locus or ubiquitinylation mediated protein degradation of the target protein, and hence the fusion protein) are intact. Hence, it provides a more faithful pattern of reported specific gene expression particularly in relation to transcriptional regulation than the heterologous over-expression of similar fusion proteins (for example, as encoded and expressed from blastomere microinjected recombinant plasmids or mRNAs). However, the creation of mCherry C-terminal fusions of endogenous genes may also compromise the function of the derived protein (post-translation). This is because the mCherry protein itself has a molecular weight of ~27kDa and thus, it could potentially interfere with the folding

and/or function of the tagged protein partner and result in its rapid degradation. Meaning, it might not be possible to detect any mCherry derived fluorescence and could potentially result in a target gene specific loss-of-function phenotype. It is too soon in the microinjection optimisation process to know if this is a problem with the *Wwc2* and *Mapk13* specific strategies described in this thesis but it remains a possibility that should be considered going forward.

In the previously referenced paper, describing the successful fluorescent tagging of several endogenous genes in preimplantation mouse embryos (representing the technical foundation of this Master's thesis project), the authors also described the generation of corresponding transgenic reporter mouse strains, that could then be bred to permanently perpetuate the reporter line (Gu *et al.*, 2018). This is because it is possible to transfer successfully genome edited preimplantation stage embryos/blastocysts to the uteri of pseudo-pregnant foster female mice. Therefore, they may continue their post-implantation development to term and in so doing transfer the edited genome sequence to the germline. The resulting transgenic adult mice can then be bred in any desired manner to propagate the fluorescent endogenous gene fusion reporter system. Moreover, using this strategy, it is possible to first check and verify the successful editing of the genome of preimplantation embryos leading to the creation of the fluorescent endogenous fusion reporter gene, prior to uterine transfer (either by directly detecting fluorescence if the endogenous gene is expressed during preimplantation development, or taking a single cell biopsy and confirming genome editing by conventional genotyping of isolated genomic DNA). Therefore, it is possible to generate male stud mice that are homozygous for a specific gene fluorescent reporter and can be bred with wild-type female mice to result in progeny embryos/offspring and expressing the desired gene specific reporter that can be appropriately studied. Moreover, if two different specific gene fluorescent reporters mouse strains are interbred (*e.g.* one specific gene tagged with mCherry and the other with EGFP), double fluorescent reporter gene mouse transgenic strains could also be generated (*i.e.* studying the expression dynamics of two gene/proteins at one time). Thus, the generation of such transgenic endogenous gene fusion reporter mouse strains can then be used to study the expression of any gene in any developing or adult tissue, in health and disease. This strategy is also applicable to generating CRISPR-Cas9 genetic nulls by omitting the inclusion of dsDNA HDR templates in the initial 2-cell stage preimplantation mouse embryo microinjections. Alternatively, it can be modified to cause insertion of

alternative heterologous DNA fragments (for example to generate conditional null alleles) using suitably modified dsDNA HDR templates. Furthermore, the relative ease of the generation of CRISPR-Cas9 mediated genome edited mouse transgenic strains compared to other previous strategies (*e.g.* bacterial recombineering of gene loci in BACs followed by inefficient incorporation into ES cell genomes, aggregation of modified ES cells into mouse blastocysts to form chimeras, uterine transfer and then subsequent rounds of breeding to ensure germline transmission of the transgenic DNA) also aids their dissemination amongst related research groups and facilitates more efficient scientific discovery and progress.

6. Conclusion

One of the thesis project's aim, to construct CRISPR-Cas9 reagents including *in vitro* derived RNAs (*i.e.* specific sgRNA and Cas9-streptavidin mRNA) and biotinylated recombinant dsDNA HDR repair template for candidate endogenous genes (*i.e.* *Wwc2*, *Mapk13* and *Mapk14*) was successful. It required individual steps including the cloning of the gene-specific homology arms into the pEasyFusion_mCherry plasmid (containing mCherry fluorescent coding reporter sequence) and subsequent generation of biotinylated dsDNA HDR templates. Furthermore, it entailed the cloning of target gene loci specific double stranded annealed oligos into the pX330-U6-Chimeric_BB-CBh-hSpCas9 plasmid, followed by generation of sgRNA encoding PCR product templates incorporating 5' T7-RNA polymerase promoter sequence and IVT to derive the gene specific sgRNA constructs for microinjection. Lastly, it involved the utilization of the pCS2⁺-Cas9-mSA plasmid to generate Cas9-streptavidin mRNA via IVT. The three derived CRISPR-Cas9 constructs, specific for the *Wwc2* and *Mapk13* genes, were microinjected into individual blastomeres of 2-cell embryos stage and resulting clones were assayed for the expression of mCherry derived fluorescence indicative of potentially successful genome editing. Although the embryo microinjections are still at an early stage of optimization, it is possible partial expression of an endogenously encoded *Mapk13-mCherry* fusion reporter transgene was detected. However, the project continues in the laboratory.

7. References

- Aksoy, I. *et al.* (2013). “Oct4 Switches Partnering from Sox2 to Sox17 to Reinterpret the Enhancer Code and Specify Endoderm.” *EMBO Journal* 32(7): 938–53.
doi: 10.1038/emboj.2013.31.
- Anders, C. *et al.* (2014). “Structural basis of PAM-dependent target DNA recognition by the Cas9 endonuclease.” *Nature* 513, 569–573.
doi: 10.1038/nature13579.
- Baumgartner, R. *et al.* (2010). “The WW Domain Protein Kibra Acts Upstream of Hippo in *Drosophila*.” *Developmental Cell* 18(2): 309–16.
doi: 10.1016/j.devcel.2009.12.013.
- Bora, P. *et al.* (2019). “P38-Mitogen Activated Kinases Mediate a Developmental Regulatory Response to Amino Acid Depletion and Associated Oxidative Stress in Mouse Blastocyst Embryos.” *Frontiers in Cell and Developmental Biology* 7(November): 1–16.
doi.org: 10.3389/fcell.2019.00276.
- Hogan Brigid, L., *et al.* (1994). “Growth Factors in Development: The Role of TGF-B Related Polypeptide Signalling Molecules in Embryogenesis.” *Development* 1994: 53-60.
PMID: 7579524
- Brouns, S. *et al.* (2008). “Small CRISPR RNAs guide antiviral defense in prokaryotes.” *Science* 321, 960–964.
doi: 10.1126/science.1159689.
- Cargnello, M., and Roux, P. P. (2011). “Activation and function of the MAPKs and their substrates, the MAPK-activated protein kinases.” *Microbiol. Mol. Biol. Rev.* 75, 50–83.
doi: 10.1128/MMBR.00031-10
- Cockburn, K., & Rossant, J. (2010). “Making the blastocyst: lessons from the mouse.” *Journal Of Clinical Investigation*, 120(4), 995-1003.
doi: 10.1172/JCI41229.
- Cong, L., *et al.* “Multiplex genome engineering using CRISPR/ Cas systems.” *Science* 339, 819–823 (2013).
doi: 10.1126/science.1231143.
- Cuadrado, A., Nebreda, AR. (2010). “Mechanisms and functions of p38 MAPK signalling.” *Biochem. J.* 429, 403–417.
doi:10.1042/BJ20100323
- Davis, J.R., and Tapon, N. (2019). “Hippo signalling during development.” *Development* 146.
doi: 10.1242/dev.167106.

Deltcheva, E., *et al.* (2011). “CRISPR RNA maturation by trans-encoded small RNA and host factor RNase III.” *Nature* 471, 602–607.
doi: 10.1038/nature09886.

Doudna, J.A., Charpentier, E. (2014). “Genome editing. The new frontier of genome engineering with CRISPR-Cas9.” *Science*.346(6213):1258096.
doi: 10.1126/science.1258096.

Ducibella, T. and Anderson, E. (1975). “Cell shape and membrane changes in the eight-cell mouse embryo: prerequisites for morphogenesis of the blastocyst.” *Dev. Biol.* 47, 45-58.
doi: 10.1016/0012-1606(75)90262-6.

Eckert, J. *et al.* (2004). “Specific PKC isoforms regulate blastocoel formation during mouse preimplantation development.” *Developmental Biology*, 274(2): 384-401.
doi: 10.1016/j.ydbio.2004.07.027.

Frankenberg, S., *et al.* (2011). “Primitive endoderm differentiates via a three-step mechanism involving Nanog and RTK signaling.” *Developmental Cell*, 21(6): 1005-1013.
doi: 10.1016/j.devcel.2011.10.019.

Gasiunas, G., *et al.* (2012). “Cas9- crRNA ribonucleoprotein complex mediates specific DNA cleavage for adaptive immunity in bacteria.” *Proc. Natl. Acad. Sci. U.S.A.* 109, E2579–E2586.
doi: 10.1073/pnas.1208507109.

Genevet, A., *et al.* (2010). “Kibra Is a Regulator of the Salvador/Warts/Hippo Signaling Network.” *Developmental Cell* 18(2): 300–308.
doi: 10.1016/j.devcel.2009.12.011.

Goldberg, J.M., *et al.* (2007). “In vitro fertilization update.” *Cleve Clin J Med.* 74(5):329–338.
doi: 10.3949/ccjm.74.5.329.

Gu, B., *et al.* (2018). “Efficient generation of targeted large insertions by microinjection into two-cell-stage mouse embryos.” *Nature Biotechnology*, 36(7), 632–637.
doi: 10.1038/nbt.4166.

Guo, G., *et al.* (2010). “Resolution of cell fate decisions revealed by single-cell gene expression analysis from zygote to blastocyst.” *Developmental Cell*, 18(4): 675-685.
doi: 10.1016/j.devcel.2010.02.012.

Haft, D .H., *et al.* (2005). “A guild of 45 CRISPR-associated (Cas) protein families and multiple CRISPR/Cas subtypes exist in prokaryotic genomes.” *PLOS Comput. Biol.* 1, e60.
doi: 10.1371/journal.pcbi.0010060.

Han, Q., *et al.* (2018). “WWC3 inhibits epithelial-mesenchymal transition of lung cancer by activating Hippo-YAP signaling.” *Onco Targets Ther* 11, 2581-2591.
doi: 10.2147/OTT.S162387.

Hirate, Y., *et al.* (2013). “Polarity-dependent distribution of Angiomin localizes Hippo signaling in preimplantation embryos.” *Current Biology*, 23(13): 1181-1194.
doi: 10.1016/j.cub.2013.05.014.

Hirate, Y., *et al.* (2015). “Par-aPKC-dependent and - independent mechanisms cooperatively control cell polarity, Hippo signaling, and cell positioning in 16-cell stage mouse embryos.” *Development, Growth and Differentiation*, 57(8): 544-556.
doi: 10.1111/dgd.12235.

Hsu, P. D., *et al.* (2014). “Development and applications of CRISPR-Cas9 for genome engineering.” *Cell* 157, 1262–1278.
doi: 10.1016/j.cell.2014.05.010.

Chazaud, C., *et al.* (2006). “Early Lineage Segregation between Epiblast and Primitive Endoderm in Mouse Blastocysts through the Grb2-MAPK Pathway.” *Developmental Cell*, 10(5), 615-624.
doi: 10.1016/j.devcel.2006.02.020.

Chazaud, C., & Yamanaka, Y. (2016). “Lineage specification in the mouse preimplantation embryo.” *Development*, 143(7), 1063-1074.
doi: 10.1242/dev.128314.

Christian, M. *et al.* (2010). Targeting DNA double-strand breaks with TAL effector nucleases. *Genetics* 186, 757–761.
doi: 10.1534/genetics.110.120717.

Iden, S., Collard, J.G. (2008). “Crosstalk between small GTPases and polarity proteins in cell polarization.” *Nature Reviews Molecular Cell Biology*, 9(11): 846-859.
doi: 10.1038/nrm2521.

Ishino, Y. *et al.* (1987). “Nucleotide sequence of the iap gene, responsible for alkaline phosphatase isozyme conversion in Escherichia coli, and identification of the gene product.” *J. Bacteriol.* 169, 5429–5433.
doi: 10.1128/jb.169.12.5429-5433.1987.

Jinek, M. *et al.* (2012). “A programmable dual-RNA–guided DNA endonuclease in adaptive bacterial immunity.” *Science* 337, 816–821.
doi: 10.1126/science.1225829.

Jinek, M. *et al.* (2013). “RNA-programmed genome editing in human cells.” *eLife* 2, e00471.
doi: 10.7554/eLife.00471.

Johnson, M.H. (2009). “From mouse egg to mouse embryo: polarities, axes and tissues.” *Annual Review of Cell and Developmental Biology*, 25: 483-512.
doi:10.1146/annurev.cellbio.042308.113348.

Kim, Y. G. *et al.* (1996). “S. Hybrid restriction enzymes: zinc finger fusions to Fok I cleavage domain.” *Proc. Natl. Acad. Sci. U. S. A.* 93, 1156–1160.
doi: 10.1073/pnas.93.3.1156.

Korotkevich, E. *et al.* (2017). “The Apical Domain Is Required and Sufficient for the First Lineage Segregation in the Mouse Embryo.” *Dev Cell*. 40(3):235-247.e7.
doi: 10.1016/j.devcel.2017.01.006.

Krupa, M. *et al.* (2014). “Allocation of Inner Cells to Epiblast vs Primitive Endoderm in the Mouse Embryo Is Biased but Not Determined by the Round of Asymmetric Divisions (8→16- and 16→32-Cells).” *Developmental Biology* 385(1): 136–48.
doi: 10.1016/j.ydbio.2013.09.008.

Leung, C. Y., & Zernicka-Goetz, M. (2013). “Angiomotin prevents pluripotent lineage differentiation in mouse embryos via Hippo pathway-dependent and -independent mechanisms.” *Nature Communications*, 4(1).
doi: 10.1038/ncomms3251.

Makarova, K.S. *et al.* (2006). “A putative RNA-interference-based immune system in prokaryotes: Computational analysis of the predicted enzymatic machinery, functional analogies with eukaryotic RNAi, and hypothetical mechanisms of action.” *Biol. Direct* 1, 7.
doi: 10.1186/1745-6150-1-7.

Marikawa, Y. and Alarcón, V. B. (2009). “Establishment of trophectoderm and inner cell mass lineages in the mouse embryo. “, *Molecular Reproduction and Development*, 76(11), pp. 1019–1032.
doi: 10.1002/mrd.21057.

Mihajlović, A. I., & Bruce, A. W. (2017). “The first cell-fate decision of mouse preimplantation embryo development: integrating cell position and polarity.” *Open Biology*, 7(11).
doi: 10.1098/rsob.170210.

Mojica, F.J. *et al.* (2000). “Biological significance of a family of regularly spaced repeats in the genomes of Archaea, Bacteria and mitochondria.” *Mol. Microbiol.* 36, 244–246.
doi: 10.1046/j.1365-2958.2000.01838.x.

Morris, S. A. *et al.* (2010). “Origin and Formation of the First Two Distinct Cell Types of the Inner Cell Mass in the Mouse Embryo.” *Proceedings of the National Academy of Sciences of the United States of America* 107(14): 6364–69.
doi: 10.1073/pnas.0915063107.

Morris, S.A., *et al.* (2012). “Developmental plasticity is bound by pluripotency and the Fgf and Wnt signaling pathways.” *Cell Reports*, 2(4): 756-765.
doi: 10.1016/j.celrep.2012.08.029.

Natale, D.R. *et al.* (2004). “p38 MAPK signaling during murine preimplantation development.” *Dev. Biol.* 268, 76–88.
doi: 10.1016/j.ydbio.2003.12.011.

- Nguyen, A.L., and Schindler, K. (2017). “Specialize and Divide (Twice): Functions of Three Aurora Kinase Homologs in Mammalian Oocyte Meiotic Maturation.” *Trends Genet* 33, 349-363.
doi: 10.1016/j.tig.2017.03.005.
- Nichols, J. *et al.* (2009). “Suppression of Erk Signalling Promotes Ground State Pluripotency in the Mouse Embryo.” *Development* 136(19): 3215–22.
doi: 10.1242/dev.038893
- Nishioka, N. *et al.* (2008). “Tead4 is required for specification of trophoctoderm in pre-implantation mouse embryos.” *Mechanisms Of Development*, 125(3-4), 270-283.
doi: 10.1016/j.mod.2007.11.002.
- Nishioka, N. *et al.* (2009). “The Hippo Signaling Pathway Components Lats and Yap Pattern Tead4 Activity to Distinguish Mouse Trophoctoderm from Inner Cell Mass.” *Developmental Cell* 16, 398–410.
doi: 10.1016/j.devcel.2009.02.003.
- Ohnishi, Y. *et al.* (2014). “Cell-to-cell expression variability followed by signal reinforcement progressively segregates early mouse lineages.” *Nature Cell Biology*, 16(1): 27-37.
doi: 10.1038/ncb2881.
- Plusa, B. *et al.* (2005). “Downregulation of Par3 and aPKC function directs cells towards the ICM in the preimplantation mouse embryo.” *J. Cell Sci.* 118:505–515.
doi: 10.1242/jcs.01666.
- Plusa, B. *et al.* (2008). “Distinct sequential cell behaviours direct primitive endoderm formation in the mouse blastocyst.” *Development*, 135(18), 3081-3091.
doi: 10.1242/dev.021519.
- Remy, G. *et al.* (2010). “Differential activation of p38MAPK isoforms by MKK6 and MKK3.” *Cell. Signal.* 22, 660–667.
doi: 10.1016/j.cellsig.2009.11.020.
- Saiz, N., Plusa, B. (2013). “Early cell fate decisions in the mouse embryo.” *Reproduction*. 145(3):R65-80.
doi: 10.1530/REP-12-0381.
- Saiz, N. *et al.* (2016). “Asynchronous Fate Decisions by Single Cells Collectively Ensure Consistent Lineage Composition in the Mouse Blastocyst.” *Nature Communications* 7:13463.
doi: 10.1038/ncomms13463.
- Sanders, Jessica R., and Keith T. Jones. (2018). “Regulation of the Meiotic Divisions of Mammalian Oocytes and Eggs.” *Biochemical Society Transactions* 46(4): 797–806.
doi: 10.1042/BST20170493.

Sasaki, H. (2010). “Mechanisms of trophectoderm fate specification in preimplantation mouse development: Specification of trophectoderm fate.” *Development, Growth & Differentiation* 52, 263–273.

doi: 10.1111/j.1440-169X.2009.01158.

Sasaki, H. (2017). “Roles and regulations of Hippo signaling during preimplantation mouse development.” *Development, Growth & Differentiation*, 59(1), 12-20.

doi: 10.1111/dgd.12335.

Schultz, R. M. (2002). “The molecular foundations of the maternal to zygotic transition in the preimplantation embryo.” *Human Reproduction Update*, 8(4), 323-331.

doi: 10.1093/humupd/8.4.323 .

Sternberg, S. H. *et al.* (2014). “DNA interrogation by the CRISPR RNA-guided endonuclease Cas9.” *Nature* 507, 62–67.

doi: 10.1038/nature13011.

Sutherland, Ann E. *et al.* (1990). “Inner Cell Allocation in the Mouse Morula: The Role of Oriented Division during Fourth Cleavage.” *Developmental Biology* 137(1): 13–25.

doi: 10.1016/0012-1606(90)90003-2.

Tarkowski, A. (1961). “Mouse Chimæras Developed from Fused Eggs.” *Nature* 190, 857–860.

doi: 10.1038/190857a0.

Tarkowski, A. K. (1959). “Experiments on the development of isolated blastomeres of mouse eggs.” *Nature*, 184(4695), pp. 1286–1287.

doi: 10.1038/1841286a0.

Thamodaran, V., and Bruce, A.W. (2016). “p38 (Mapk14/11) occupies a regulatory node governing entry 554 into primitive endoderm differentiation during preimplantation mouse embryo development.” *Open 555 Biol* 6.

doi: 10.1098/rsob.160190.

Vinot, S. *et al.* (2004). “Two PAR6 proteins become asymmetrically localized during establishment of polarity in mouse oocytes.” *Curr. Biol.* 14:52–55.

doi: 10.1016/j.cub.2004.02.061.

Vinot S. *et al.* (2005). “Asymmetric distribution of PAR proteins in the mouse embryo begins at the 8---cell stage during compaction.” *Dev. Biol.* 282:307–319.

doi: 10.1016/j.ydbio.2005.03.001.

Virnicchi, G. *et al.* (2020). “Wwc2 Is a Novel Cell Division Regulator During Preimplantation Mouse Embryo Lineage Formation and Oogenesis.” *Front Cell Dev Biol.* 8:857.

doi: 10.3389/fcell.2020.00857.

Wassarman, P. M. *et al.* (2013). “Biogenesis of the Mouse Egg’s Extracellular Coat, the Zona Pellucida.” In *Current Topics in Developmental Biology*, Academic Press Inc., 243–66.

doi: 10.1016/B978-0-12-416024-8.00009-X.

- Wennmann, D. O. *et al.* (2014). “Evolutionary and molecular facts link the WWC protein family to Hippo signaling.” *Mol. Biol. Evol.* 31, 1710–1723.
doi: 10.1093/molbev/msu115.
- White, M. D. *et al.* (2018). “Instructions for Assembling the Early Mammalian Embryo.” *Developmental Cell*, 45(6), 667-679.
doi: 10.1016/j.devcel.2018.05.013.
- Xiao, L. *et al.* (2011). “KIBRA regulates Hippo signaling activity via interactions with large tumor suppressor kinases.” *J Biol Chem* 286, 7788-7796.
doi: 10.1074/jbc.M110.173468.
- Yagi, R. *et al.* (2007). “Transcription factor TEAD4 specifies the trophectoderm lineage at the beginning of mammalian development.” *Development*, 134(21): 3827-3836.
doi: 10.1242/dev.010223.
- Yamanaka, Yojiro, Fredrik Lanner, and Janet Rossant. (2010.) “FGF Signal-Dependent Segregation of Primitive Endoderm and Epiblast in the Mouse Blastocyst.” *Development* 137(5): 715–24.
doi: 10.1242/dev.043471.
- Zernicka-Goetz, M. *et al.* (2009). “Making a firm decision: multifaceted regulation of cell fate in the early mouse embryo. *Nat Rev Genet* 10, 467–477.
doi: 10.1038/nrg2564.
- Zhang, Y. *et al.* (2017). “WWC2 is an independent prognostic factor and prevents invasion via Hippo signalling in hepatocellular carcinoma. “ *J Cell Mol Med* 21, 3718-3729.
doi: 10.1111/jcmm.13281.
- Zhao, B. *et al.* (2007). “Inactivation of YAP oncoprotein by the Hippo pathway is involved in cell contact inhibition and tissue growth control.” *Genes & Development* 21, 2747–2761.
doi: 10.1101/gad.1602907.

8. Appendix

Created with SnapGene®

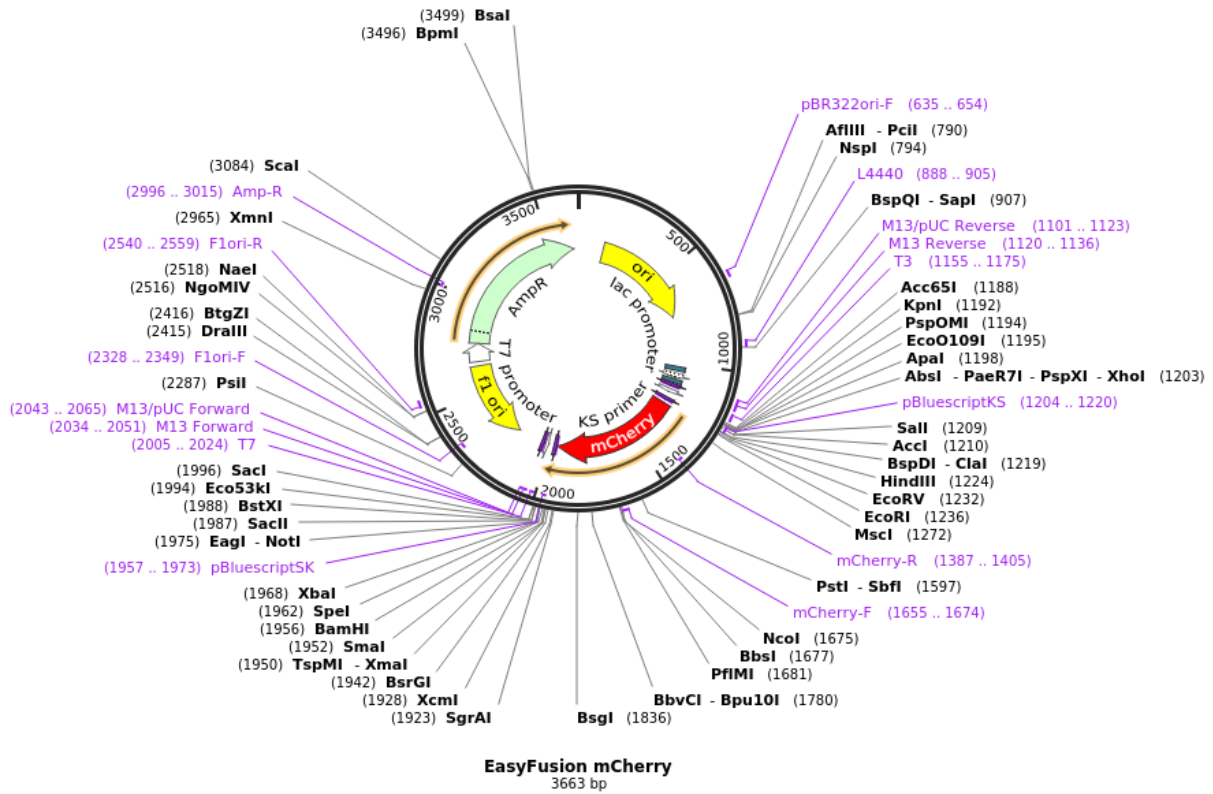


Figure 33. The map of pEasyFusion-mCherry recombinant plasmid. Taken from <https://www.addgene.org/112849/>, 4.12.2020).

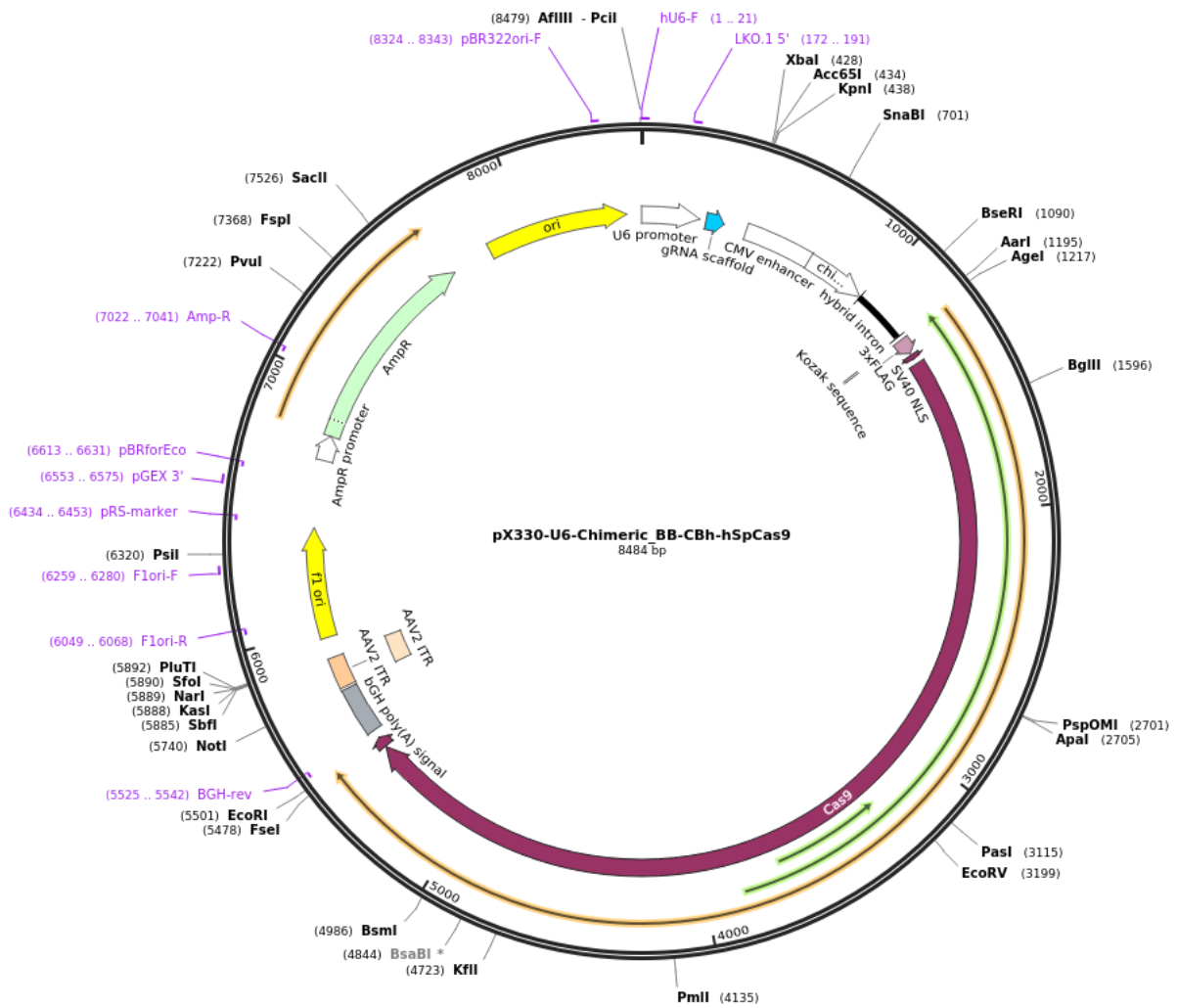


Figure 34. The map of pX330-U6-Chimeric_BB-CBh-hSpCas9. Taken from <https://www.addgene.org/42230/>, 4.12.2020).

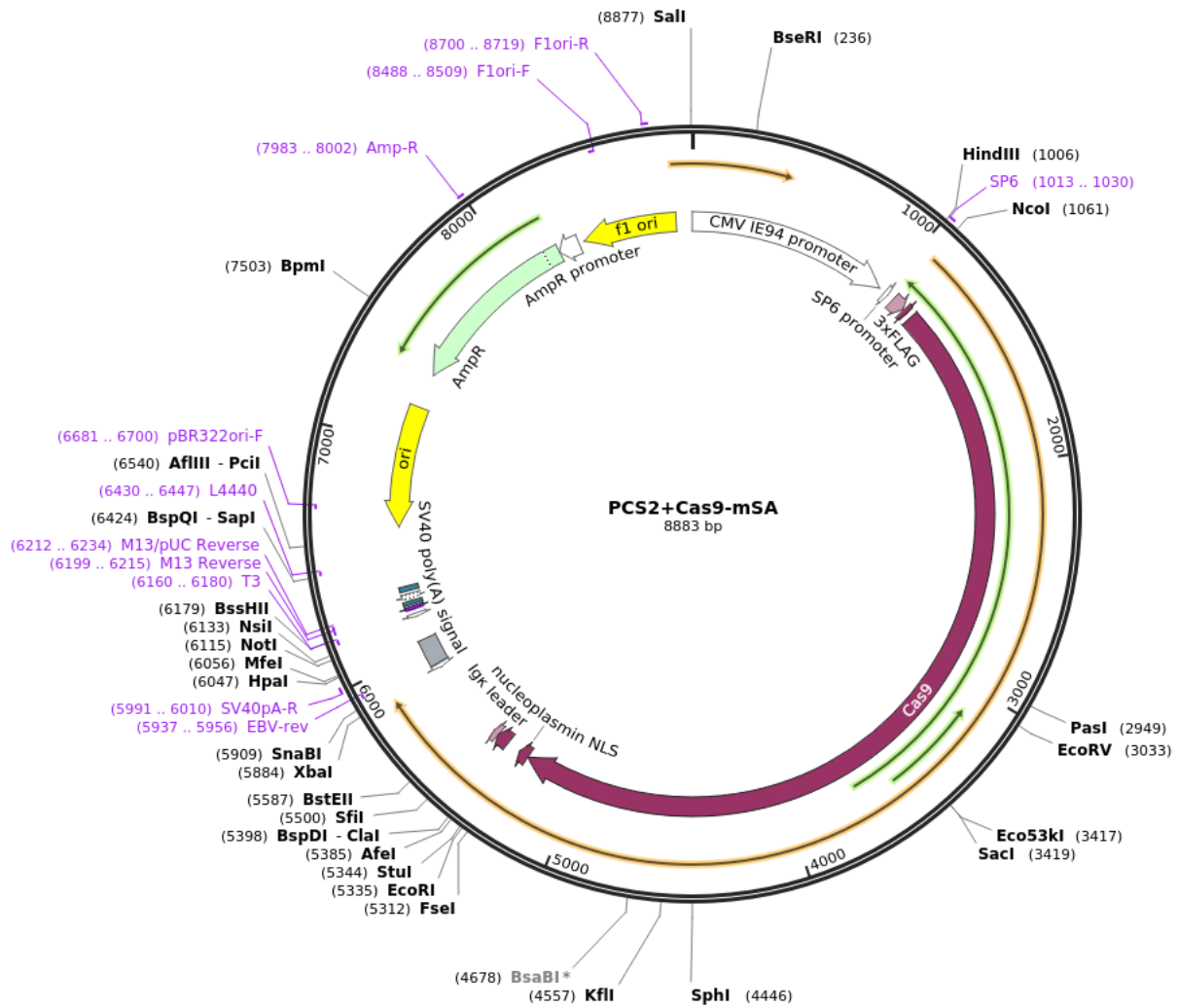


Figure 35. The map of PCS2+Cas9-mSA plasmid. Taken from <https://www.addgene.org/103882/>, 4.12.2020).